NADPH Oxidase 2–Derived Reactive Oxygen Species Promote CD8$^+$ T Cell Effector Function

Jing Chen,*[,1] Chao Liu,*[,1] Anna V. Chernatynskaya,* Brittney Newby,* Todd M. Brusko,* Yuan Xu,[†] Jessie M. Barra,[‡] Nadine Morgan,[‡] Christopher Santarlas,[§] Westley H. Reeves,[†] Hubert M. Tse,[‡,2] Jennifer W. Leiding,[¶,‖] and Clayton E. Mathews*

Oxidants participate in lymphocyte activation and function. We previously demonstrated that eliminating the activity of NADPH oxidase 2 (NOX2) significantly impaired the effectiveness of autoreactive CD8$^+$ CTLs. However, the molecular mechanisms impacting CD8$^+$ T cell function remain unknown. In the present study, we examined the role of NOX2 in both NOD mouse and human CD8$^+$ T cell function. Genetic ablation or chemical inhibition of NOX2 in CD8$^+$ T cells significantly suppressed activation-induced expression of the transcription factor T-bet, the master transcription factor of the Tc1 cell lineage, and T-bet target effector genes such as IFN-γ and granzyme B. Inhibition of NOX2 in both human and mouse CD8$^+$ T cells prevented target cell lysis. We identified that superoxide generated by NOX2 must be converted into hydrogen peroxide to transduce the redox signal in CD8$^+$ T cells. Furthermore, we show that NOX2-generated oxidants deactivate the tumor suppressor complex leading to activation of RheB and subsequently mTOR complex 1. These results indicate that NOX2 plays a nonredundant role in TCR-mediated CD8$^+$ T cell effector function. ***The Journal of Immunology*****, 2024, 212: 258–270.**

CD8$^+$ CTLs play vital roles in antitumor immunity, elimination of intracellular infections, and the pathogenesis of autoimmune diseases, including type 1 diabetes (T1D) (1, 2). Activation of CD8$^+$ T cells leads to cell expansion, differentiation, and downstream production of proinflammatory cytokines and cytotoxic factors, which are critical to induce cell death in Ag-bearing target cells. During CD8$^+$ T cell activation, multiple factors function collaboratively to control the master transcription factors that regulate effector function (3–5). Reactive oxygen species (ROS), a group of low-m.w., highly reactive molecules containing oxygen (6), have been proposed as one of the signal transducers for CD8$^+$ T cell activation and CTL differentiation (7, 8).

At high concentrations, ROS can be toxic and can participate in pathologies; however, regulated ROS production controls cellular functions by mediating redox signaling (6, 9, 10). Specific enzyme families, such as the NADPH oxidases (9), can modulate redox signal transduction through production of ROS. NADPH oxidase 2 (NOX2) is expressed in a wide variety of tissues/cell types and is the free radical source of the "respiratory burst" in neutrophils and macrophages to destroy microbes and as a biological second messenger for signal transduction within lymphocytes (9, 10). NOX2 is a six-subunit enzyme complex (11). In resting cells, the cytochrome resides in membranes, whereas the remining four subunits, including p47^{phox} (*Ncf1*), are complexed in the cytoplasm (12). In response to stimulation, p47^{phox} is phosphorylated and organizes assembly of the active subunit enzyme. We have reported that NOX2 regulates CD4$^+$ T cell differentiation by promoting Th1 responses (13), a finding confirmed by subsequent studies with human samples (14). In addition, we have observed a CD8$^+$ T cell intrinsic role of NOX2 that is essential for autoimmune diabetes initiation (8). Therefore, our data as well as those from other groups support an important role of NOX2 in adaptive immune function in addition to the well-established role of NOX2 in innate immunity (15, 16). The goal of the present study is to elucidate the mechanisms of NOX2 in regulating CD8$^+$ T cell effector function.

T1D is caused by an autoimmune-mediated destruction of insulin-producing β cells (17–22). CTLs are considered the final effector cells

*Department of Pathology, Immunology and Laboratory Medicine, University of Florida, Gainesville, FL; [†]Department of Medicine, University of Florida, Gainesville, FL; [‡]Department of Microbiology, University of Alabama at Birmingham, Birmingham, AL; [§]Morsani College of Medicine, University of South Florida, Tampa, FL; [¶]Division of Allergy and Immunology, Department of Pediatrics, Johns Hopkins University, Baltimore, MD; and [‖]Institute for Clinical and Translational Research, Johns Hopkins All Children's Hospital, St. Petersburg, FL

[1]J.C. and C.L. contributed equally to this work.

[2]Current address: Department of Microbiology, Molecular Genetics & Immunology, University of Kansas Medical Center, Kansas City, KS.

ORCIDs: 0000-0001-8008-8062 (J.C.); 0000-0002-8179-0010 (A.V.C.); 0000-0001-8648-4349 (B.N.); 0000-0003-2878-9296 (T.M.B.); 0000-0001-7705-6043 (N.M.); 0000-0001-5861-7597 (H.M.T.); 0000-0002-8817-6355 (C.E.M.).

Received for publication September 19, 2022. Accepted for publication November 7, 2023.

This work was supported by a research grant from the Juvenile Diabetes Research Foundation; National Institutes of Health Grants R01 DK074656 (to C.E.M.), UC4 DK104194 (to C.E.M.), P01 AI042288 (to C.E.M.), and F30 DK105788 (to B.N.); and grants from Horizon Therapeutics (to J.W.L.) and the Sebastian Family Endowment for Diabetes Research (to C.E.M.).

J.C. researched the data and wrote the manuscript. C.L. researched the data and wrote the manuscript. A.V.C. researched the data and reviewed and edited the manuscript. B.N. researched the data and reviewed and edited the manuscript. T.M.B. contributed to discussion and reviewed and edited the manuscript. Y.X. researched the data and reviewed and edited the manuscript. J.M.B. and N.M. researched the data and reviewed and edited the manuscript. C.S. researched the data and reviewed and edited the manuscript. W.H.R. contributed to discussion and reviewed and edited the manuscript. H.M.T. conceived of the study and reviewed and edited the manuscript. J.W.L. researched the data and reviewed and edited the manuscript. C.E.M. conceived of the study and wrote the manuscript.

Address correspondence and reprint requests to Prof. Clayton E. Mathews, Department of Pathology, Immunology and Laboratory Medicine, The University of Florida College of Medicine, University of Florida, P.O. Box 100275, Gainesville, FL 32610-0275. E-mail address: clayton.mathews@pathology.ufl.edu

The online version of this article contains supplemental material.

Abbreviations used in this article: BAL, British anti-Lewisite; CGD, chronic granulomatous disease; CML, cell-mediated lymphocytoxicity; Eomes, eomesodermin; MFI, median fluorescence intensity; mTORc1, mammalian target of rapamycin complex 1; NOX2, NADPH oxidase 2; PAO, phenylarsine oxide; ROS, reactive oxygen species; SOD1, superoxide dismutase 1; T1D, type 1 diabetes; TdR, [^{3}H]-thymidine.

This article is distributed under The American Association of Immunologists, Inc., Reuse Terms and Conditions for Author Choice articles.

Copyright © 2024 by The American Association of Immunologists, Inc. 0022-1767/24/$37.50

https://doi.org/10.4049/jimmunol.2200691

of β-cell death in the NOD mouse (18, 23–26). CTLs induce β-cell death by using proinflammatory cytokines and cytotoxic effector molecules such as IFN-γ and TNF-α, perforin, and granzyme B. We reported that NOX2-produced ROS contribute to the onset of diabetes in NOD mice using a NOD strain that encodes a nonfunctional NOX2 enzyme (NOD-*Ncf1*^{m1J}) (8, 13, 27). Adoptive transfer of CTLs from NOX2-deficient NOD-*Ncf1*^{m1J} donors into NOX2-intact recipients (NOD-*Scid*) resulted in a delayed onset of diabetes, indicating that NOX2 activity within the CTL is required for pathogenesis (8).

Production of proinflammatory cytokines and effector molecules as well as cytotoxic activity of human and mouse CD8$^+$ T cells are shown in the present study to be blocked by genetic ablation or pharmacological inhibition of NOX2. Hydrogen peroxide derived from NOX2 promoted CD8$^+$ T cell effector function by enhancing the production of T-bet, the master transcription factor of the Tc1 cell lineage and driver of effector genes such as IFN-γ and granzyme B. ROS affected T-bet by regulating mammalian target of rapamycin complex 1 (mTORc1) activity via RheB-GTP levels through the redox-sensitive Tsc1/Tsc2 signaling complex. Collectively, these findings define a mechanism by which NOX2 functions in CD8$^+$ T cells and highlights the significance of redox signaling in CTL-mediated diseases such as T1D.

Materials and Methods

Animals

NOD-*Ncf1*^{m1J} mice, described previously (8, 13, 27), were bred and maintained at the University of Florida. All other mouse strains [NOD/ShiLtJ (NOD), NOD.CB17-*Prkdc*^{scid}/J (NOD-*Scid*), NOD.Cg-*Rag1*^{tm1Mom}-*Thy1*$^{\alpha/\alpha}$-Tg (TcraAI4)^{1Dvs}/DvsJ (NOD.AI4α-*Rag1*$^{-/-}$), NOD.Cg-*Rag1*^{tm1Mom} (TcrbAI4)^{1Dvs}/DvsJ (NOD.AI4β-*Rag1*$^{-/-}$) as well as C57BL6/J (B6) and B6(Cg)-*Ncf1*^{m1J}/J (B6-*Ncf1*^{m1J}) mice] were purchased from The Jackson Laboratory (Bar Harbor, ME). F1 hybrid progeny were developed from outcrosses of NOD.AI4α-*Rag1*$^{-/-}$ to NOD.AI4β-*Rag1*$^{-/-}$ and referred to as NOD.AI4α/β-*Rag1*$^{-/-}$. Female mice were used for all experiments. All mice used in this study were housed in specific pathogen-free facilities, and all procedures were approved by institution animal care and use committees of the University of Florida, the University of Alabama at Birmingham, and the University of Kansas Medical Center.

Human subjects

The institutional review board of the University of Florida approved all studies with human samples. Leukopaks from healthy donors (50% female, aged 16–25 y, median age 19 y) were purchased from Life South Blood Centers. PBMCs were isolated using the Ficoll gradient method.

Materials

Chemicals were purchased from Sigma-Aldrich. HRP-conjugated secondary Abs were purchased from Santa Cruz Biotechnology. Fluorescently labeled Abs used for flow cytometry analysis with either a BD LSRFortessa or Cytek Aurora are listed below.

Purification and cell culture of mouse CD8$^+$ T cells

Spleens from age-matched NOD, NOD-*Ncf1*^{m1J} B6, and B6-*Ncf1*^{m1J} females were collected, homogenized to a single-cell suspension, and subjected to hemolysis with Gey's solution (28). CTLs were negatively selected using paramagnetic beads following column selection (CD8$^+$ T cell isolation kit; Miltenyi Biotec). Purity was greater than 90% and confirmed on a BD LSRFortessa (BD Biosciences). Purified CD8$^+$ cells were cultured in complete DMEM. All cultures using mouse T cells were performed in complete DMEM (low glucose [5.5 mM] DMEM [Corning Cellgro] containing 10% FBS [HyClone Laboratories], HEPES buffer, gentamicin [Gemini], MEM Non-Essential Amino Acids Solution [Life Technologies] and 2-ME).

Immunospin trapping and immunofluorescence

Macromolecular-centered free radicals were detected after stimulation of purified NOD and NOD.*Ncf1*^{m1J} CD8$^+$ T cells with α-CD3 (clone 145-2C11, 0.1 μg/ml; BD Pharmingen) and α-CD28 (clone 37.51, 1 μg/ml; BD Pharmingen) in the presence of 5,5-dimethyl-1-pyrroline *N*-oxide (DMPO; 1 mmol/L) in tissue culture–treated chamber slides. After 24 h, cells were fixed in 4% paraformaldehyde in PBS, permeabilized with 0.1% Triton X-100 + 0.1% Tween in PBS, blocked with 10% BSA in PBS, and incubated with chicken IgY anti-DMPO (20 μg/ml) and rat anti-mouse CD8a (1:250; SouthernBiotech). DMPO adducts were detected with Alexa Fluor 488–conjugated goat anti-chicken IgY secondary Ab (1:400; Jackson ImmunoResearch). CD8$^+$ T cells were identified with Cy3-conjugated donkey anti-rat secondary Ab (1:500; Jackson ImmunoResearch). Images were obtained with an Olympus IX81 inverted microscope using a 403 objective and analyzed with cellSens Dimension version 1.9 imaging software. For quantitation of fluorescence intensity, three to six images were obtained for each data point. Each image was collected at the same exposure time, adjusted to the same intensity level for standardization, and the fluorescence intensity was measured using ImageJ software (National Institutes of Health).

CD8$^+$ T cell proliferation

CD8$^+$ T cells (1×10^5) were used for proliferation after stimulation with plate-bound α-CD3ε (0.1 μg/ml) and α-CD28 (1 μg/ml) or beads conjugated with α-CD3ε and α-CD28 in the presence or absence of 200 μM apocynin (EMD Millipore). This dose of apocynin was used on the basis of dose–response curves using increasing concentrations of apocynin (0–300 μM) and analyzing viability by flow cytometry (Live/Dead Near IR; Thermo Fisher) (Supplemental Fig. 2A), and IFN-γ levels were analyzed by ELISA (BD Biosciences) (Supplemental Fig. 2B). To examine the specific ROS that influence activation, CD8$^+$ T cells were incubated with superoxide dismutase 1 (SOD1; 100 U/ml), or catalase (1000 U/ml), or IL-2 (25 U/ml) during α-CD3ε and α-CD28 bead stimulation. Cell proliferation was measured by [^{3}H]-thymidine (TdR) incorporation as performed previously (13).

Detection of cytokine production and secretion by mouse CD8$^+$ T cells

Purified CD8$^+$ T cells (5×10^5) from NOD, NOD-*Ncf1*^{m1J}, and B6 mice were activated with plate-bound α-CD3ε and α-CD28 or PMA (50 ng/ml) plus ionomycin (1 μg/ml) for a total of 72 h, as previously described (29, 30). Cells were stained with Pacific Blue–labeled α-CD8 (53-6.7; BioLegend) and fixed and then permeabilized prior to being stained with fluorescently labeled Abs to IFN-γ–FITC (XMG1.2; BD Biosciences), granzyme B–PE (NGZB; eBioscience), and T-bet–allophycocyanin (4B10, BioLegend). Data were collected using a BD LSRFortessa by gating on CD8$^+$ T cells and then producing histograms of the intracellular targets. Isotype controls and fluorescence-minus-one conditions were used to set gates for marker positivity for the protein of interest.

For Ag-specific activation of mouse AI4 T cells, NOD.AI4α/β-*Rag1*$^{-/-}$ splenocytes were activated with 0.1 μM mimotope (amino acid sequence YFIENYLEL) and 25 U/ml IL-2 for 72 h (31, 32) with or without the presence of 200 μM apocynin. Cells were stained with LIVE/DEAD Fixable Near-IR to exclude dead cells, blocked with Fc block (BD Biosciences), and stained for surface markers CD3-PE-Cy5 (145-2C11; eBioscience), CD8-BV650 (53-6.7; BioLegend), CD62L-BV711 (MEL-14; BioLegend), and CD69-PerCP-Cy5.5 (H1.2F3; BD Biosciences). Then cells were fixed and permeabilized using the eBioscience FoxP3/Transcription Factor Fixation/Permeabilization kit and stained for perforin–allophycocyanin (S16009A; BioLegend), IFN-γ–FITC (XMG1.2; BD Biosciences), granzyme B–PacBlue (GB11; BioLegend), and T-bet–BV605 (4B10; BioLegend). Data were acquired on a three-laser Cytek Aurora spectral flow cytometer.

Phosflow for detection of p-S6K, p-AKT, p-ZAP70, and p-S6 was performed using splenocytes from NOD.AI4α/β-*Rag1*$^{-/-}$ mice that were activated with mimotope, mentioned above, for 30 min. Splenocytes from NOD and NOD-*Ncf1*^{m1J} mice were activated with soluble anti-CD3 (2 μg/ml, clone 145-2C11; BD Biosciences), anti-CD28 (10 μg/ml, clone 37.51; BD Biosciences), and protein G (5 μg/ml; Sigma-Aldrich) as a crosslinker for 30 min. Stimulation was stopped by adding a 1/3 volume of fixation buffer (4× stock; Invitrogen) and fixed for 30 min at room temperature, then cells were washed once with PBS, stained with LIVE/DEAD Fixable Near-IR to exclude dead cells, permeabilized with prechilled 90% methanol for 30 min on ice, blocked with Fc block as well as mouse and rabbit serum, and stained with anti-CD3-Pacific Blue (clone 17A2; BioLegend), anti-CD8-BV605 (clone 53-6.7; BioLegend), anti-CD4-BV711 (clone V4; BioLegend), anti-phospho-AKT1 (Ser473)-allophycocyanin (clone SDRNR; Thermo Fisher), and anti-p70-S6K-PE (clone 215247; R&D Systems), or anti-phospho-S6 (Ser235, Ser236)-PE (cupk43k; Thermo Fisher). Data were acquired on a three-laser Aurora spectral flow cytometer. All flow data were analyzed with FlowJo (version 7.6-10.8.0). Results were expressed as the median fluorescence intensity (MFI) ratio to activated or unstimulated isotype control when gated on live CD3$^+$CD8$^+$ cells.

Secreted IFN-γ was analyzed using CD8$^+$ T cells (5×10^4) that were stimulated with α-CD3ε and α-CD28 conjugated beads (Life Technologies). IFN-γ was detected with the BD OptEIA Mouse IFNγ ELISA Set (BD Biosciences). ELISA plates were read on a SpectraMax Multi-Mode Microplate Reader and analyzed using Softmax Pro version 5.0.1 (Molecular Devices Corp.).

Quantitative real-time PCR

Total RNA from purified $CD8^+$ T cells was isolated with TRIzol reagent (Invitrogen). cDNA was prepared using the SuperScript III First-Strand Synthesis System (Invitrogen) according to the manufacturer's protocol. Real-time quantitative PCR was performed as previously reported (33–35) using SYBR Green I (Bio-Rad Laboratories) on a Roche LightCycler 480 II. The amplification program used the following steps for all primer sets: 95°C for 10 min, followed by 45 cycles of 95°C for 30 s, 60°C for 30 s, and 72°C for 30 s. The melting curves of the PCR products were measured to ensure the specificity. Primers (Supplemental Table I) were designed using qPrimerDepot (National Institutes of Health).

Mouse cell-mediated lymphocytoxicity assays

Cell-mediated lymphocytoxicity (CML) assays were performed as described previously (19, 21, 36, 37). Briefly, splenocytes from NOD.AI4α/β-*Rag1*$^{-/-}$ mice were primed in RPMI 1640 complete media containing 25 U/ml IL-2 and 0.1 μM mimotope (amino acid sequence YFIENYLEL) for 3 d with [CTL activation phase (+)] or without [CTL activation phase (−)] 200 μM apocynin. NOD-derived NIT-1 β cells (38) were plated at 10,000 cells per well in flat-bottomed 96-well plates. NIT-1 cells were primed with 1000 U/ml IFN-γ for 24 h. The NIT-1 cells were then labeled with 1 μCi/well of ^{51}Cr (PerkinElmer) for 3 h at 37°C and cocultured with AI4 T cells at an E:T ratio of 20:1 for 16 h, with [CTL effector phase (+)] or without [CTL effector phase (−)] the presence of 200 μM apocynin. Specific lysis was calculated as described (19, 21, 36, 37).

Measurements of human $CD8^+$ T cell activation, proliferation, and molecular changes

Purified total human T cells were cultured in complete RPMI. Culture media contained the indicated concentration of apocynin. Total T cells (1×10^6) were activated with plate-bound α-CD3ε (OKT3; BioLegend) plus α-CD28 (CD28.2 RUO; BD Biosciences) at 5 μg/ml each or corresponding isotype controls for a total of 72 h. For IFN-γ detection by ELISA, media supernatants were collected at 24, 48, and 72 h, and the IFN-γ levels were determined using the BD OptEIA Human IFNγ ELISA set. For intracellular staining, cells were activated for 66 h and then restimulated with PMA (50 ng/ml) plus ionomycin (1 μg/ml) with the addition of GolgiStop (BD Biosciences) for 6 h at 37°C in a 5% CO_2 humid air incubator. Cell proliferation was measured by [^{3}H]TdR incorporation. In independent cultures, cells were stained with α-human CD8-FITC (G42-8; BD Pharmingen), CD69-BV605 (FN50; BioLegend), and CD4-PE-Cy7 (RPA-T4; eBioscience) followed by intracellular staining to detect IFN-γ-PerCP-Cy5.5 (4S.B3; BioLegend), granzyme B–Alexa Fluor 647 (GB11; BioLegend), T-bet-Pacific Blue (4B10; BioLegend), and eomesodermin (Eomes)-PE (WD1928; eBioscience). Intracellular staining was performed with the True Nuclear Transcription Factor staining kit (BioLegend) according to the manufacturer's protocol. Fluorescence was measured using a BD LSRFortessa, and results were analyzed using FlowJo version 7.6.1 software.

Leukopak PBMCs were pretreated with apocynin 400 μM, DMSO 0.04%, or were left untreated in complete RPMI for 1 h at 37°C in a CO_2 incubator. Cells were then activated with soluble α-CD3 (1 μg/ml) and α-CD28 (5 μg/ml) or isotype Abs, together with protein G (5 μg/ml; Sigma-Aldrich) as a crosslinker for 10 min at 37°C in a CO_2 incubator. At the end of activation, the reaction was stopped by immediately adding 4× fixation stock to reach 1× concentration of fixation buffer and fixed for 30 min. Samples were then stained for viability with the LIVE/DEAD Fixable Yellow Dead Cell Stain Kit (Invitrogen), blocked with Fc block (Thermo Fisher), permeabilized with ice-cold 90% methanol, and stained for surface markers CD3-eFluor 450 (UCHT1; eBioscience), CD4-FITC (RPA-T4; BioLegend), and CD8-BV711 (SK1; BioLegend), as well as intracellular molecules phospho-S6 (Ser235, Ser236)-PE (cupk43k; Thermo Fisher) and phospho-AKT1 (Ser473)-allophycocyanin (SDRNR; Thermo Fisher). Data were analyzed on a Cytek Aurora, and results were expressed as the MFI ratio to activated when gated on Live/Dead_Yellow$^-$CD3$^+$CD4$^-$ CD8$^+$ cells.

CML assays using autoreactive human $CD8^+$ T cell avatars and human-derived BetaLox5 cells as target cells

$CD8^+$ T cells were preenriched from leukopaks ($n = 3$) by negative selection (RosetteSep; STEMCELL Technologies) and then stained with CD8–allophycocyanin/Cy7 (clone SK1; BioLegend), CD45RA-PerCP/Cy5 (clone H1100; BioLegend), and CD45RO-PE/Cy7 (clone UCHL1; BioLegend). Naive $CD8^+CD45RA^+CD45RO^-$ T cells were sorted using a BD FACSAria III. Purified (91.0 ± 2.5% purity) naive $CD8^+$ T cells were activated with α-CD3/CD28 Dynabeads (Life Technologies) in the presence or absence of apocynin (200 μM). At 48 h, cells were transduced with a lentiviral vector containing an IGRP-specific, HLA-A*0201 restricted TCR, as previously described (19). After transduction, $CD8^+$ avatars were supplemented with complete RPMI (Corning Cellgro) and IL-2 (300 U/ml) with or without apocynin (200 μM) every 48 h. Transduction efficiency for the cells expanded in apocynin was 32.4%, whereas those expanded in media free of apocynin were transduced at 22.3%. After transduction, cells were expanded for an additional 7 d, and, on day 9, the cells were cryopreserved in freeze medium (90% FBS/10% DMSO). Cells were thawed and then immediately used for the CML assays. CML assays were performed as described previously using BetaLox5 (BL5) cells as target (19, 36).

Measurement of mTORc1 activity

mTORc1 activity analysis was performed using purified $CD8^+$ T cells (1×10^7) from NOD and NOD-*Ncf1*^{m1J} mice. Western blotting was used as the output assay to determine levels of the ribosomal protein S6 kinase (p-S6K) using an S6K and p-S6K Abs (Cell Signaling Technology). To assess the impact of mTORc1 inhibition, rapamycin (20 ng/ml) treatment was performed 15 min prior to polyclonal activation of T cells. For redox reagent treatment, purified $CD8^+$ T cells were exposed to either 5 μM phenylarsine oxide (PAO), 1 mM 2,3-dimercapto-1-propanol (British anti-Lewisite [BAL]), 10 μM H_2O_2, or 200 μM apocynin 15 min before activation. All treatments were performed in complete DMEM. T cells were then activated with α-CD3ε– and α-CD28–conjugated beads for 30 min. Cell lysates were then generated by sonication in radioimmunoprecipitation assay buffer and subjected to Western blot analysis for p-S6K and total S6K. Lysates were separated on 7.5% gel (Bio-Rad Laboratories) and transferred to 0.45-μm–charged PVDF membranes. Membranes were incubated overnight at 4°C with Abs against p-S6K or total S6K and then exposed to the secondary Ab conjugated to HRP. For normalization, membranes were stripped and reprobed with α-Erk1/2 (polyclonal, 137F5; Cell Signaling Technology), followed by incubation with HRP-conjugated secondary Ab. Chemiluminescence was detected, and photon signals were converted to densitometry data with a FluorChem HD2 with AlphaView software (Alpha Innotech). Activation-induced p-AKT and p-S6 activity was confirmed in these samples via Phosflow, as noted above.

Measurement of RheB-GTP levels after $CD8^+$ T cell activation by flow cytometry

Anti-RheB-GTP was purchased from NewEast Biosciences (catalog no. 26910, clone 20D11D6) and conjugated using the Pacific Blue Ab Labeling Kit (P30013; Invitrogen). Splenocytes were isolated from NOD or NOD-*Ncf1*^{m1J} mice and activated with soluble α-CD3/α-CD28 or treated with isotype Abs, as mentioned above, for 10 min, then fixed and stained with the LIVE/DEAD Fixable Yellow (LDY) Dead Cell Stain Kit (Invitrogen), permeabilized with prechilled 90% methanol, stained with conjugated Abs to RheB-GTP, CD3, CD8, pS6, p-ATK, and total RheB for analysis with a three-laser Cytek Aurora flow cytometer. RheB-GTP was analyzed in LDY$^-$ CD3$^+$CD8$^+$ population, expressed as the ratio of MFI of activated cells to that of isotype Ab-treated cells.

Statistics

Each experiment was run in triplicate with at least three independent trials. Statistical analysis was performed using GraphPad Prism (GraphPad Software) or SAS 9.2 (SAS Institute). Statistical significance between mean values was determined using the Student t test or one-way ANOVA, with $p < 0.05$ considered as significantly different.

Results

*$CD8^+$ T cells in NOD-*Ncf1^{m1J} *mice exhibit a reduced production of proinflammatory cytokines and effector molecules*

NOX2 functions in TCR signaling upon CD3 and CD28 crosslinking (8, 39), and ROS are produced during $CD8^+$ T cell activation (40). ROS production by $CD8^+$ T cells from NOD and NOD.*Ncf1*^{m1J} mice was examined using the immunospin trap DMPO after stimulation with α-CD3 and α-CD28. Similar to our previous report (8), NOD.*Ncf1*^{m1J} $CD8^+$ T cells exhibited significantly less ROS production after stimulation when compared with $CD8^+$ T cells from NOD mice (Supplemental Fig. 1).

Earlier studies led us to hypothesize that NOX2-deficient NOD-*Ncf1*^{m1J} $CD8^+$ T cells would exhibit defective effector function in vitro (8). Stimulation of NOD-*Ncf1*^{m1J} $CD8^+$ T cells with α-CD3 and α-CD28 elicited a significant reduction in IFN-γ production,

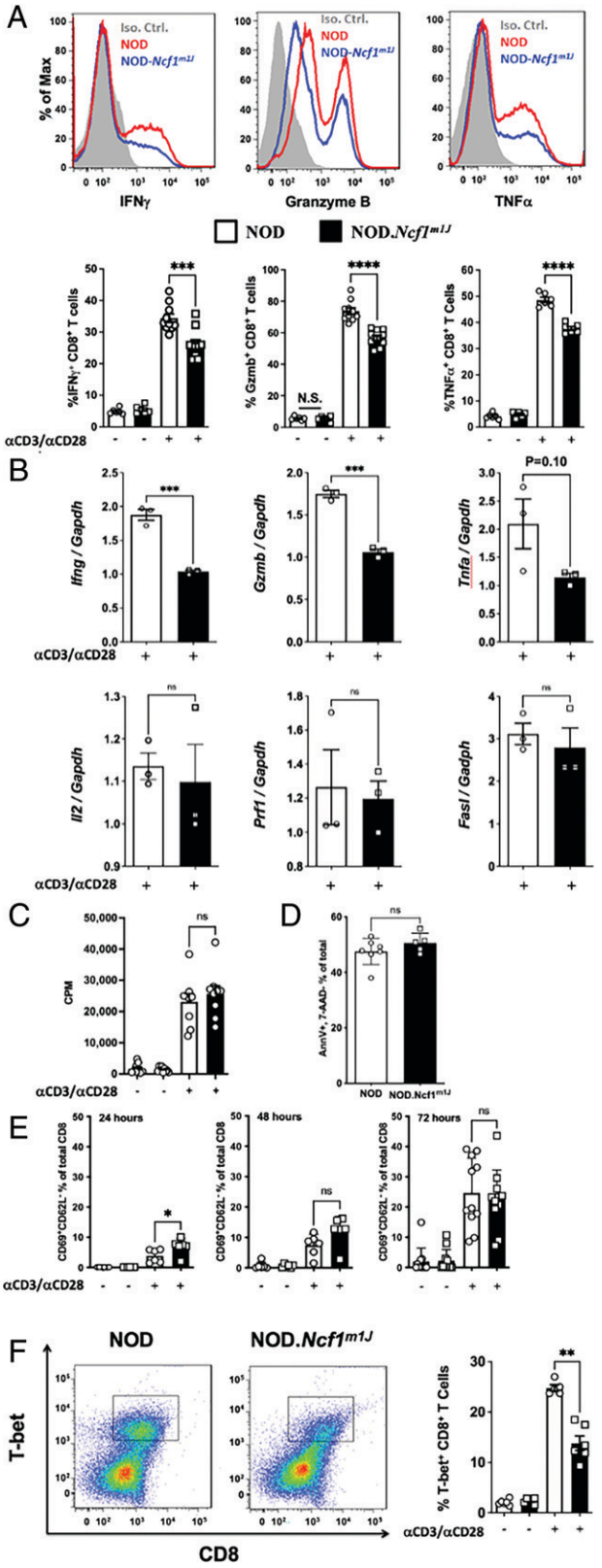

FIGURE 1. NOD-*Ncf1*^{m1J} CD8$^+$ T cells exhibit a decrease in proinflammatory cytokine and effector molecule production. (**A**) Representative histogram and the quantitation of intracellular staining in purified CD8$^+$ T cells after stimulation of NOD (red histogram or open bar) or NOD-*Ncf1*^{m1J} (blue histogram or black bar) with α-CD3/α-CD28 Abs for 72 h. Gray histogram represents the isotype control. Twelve mice were included in each group. (**B**) Real-time quantitative PCR of cytokine and effector molecule mRNA in CD8$^+$ T cells after α-CD3/α-CD28 stimulation of NOD (open bar) or NOD-*Ncf1*^{m1J} (black bar) for 48 h. PCR was performed with pooled cDNA from three mice, and results were compiled from three independent experiments performed in triplicate. (**C**) Proliferation was assessed by ^{3}H-TdR incorporation using CD8$^+$ T cells activated with α-CD3/α-CD28 for 72 h. (**D**) CD8$^+$ T cell apoptosis 72 h after α-CD3/α-CD28 activation. (**E**) Surface activation markers were detected using flow cytometry after CD8$^+$ T cells were activated with α-CD3/α-CD28 for 24, 48, and 72 h. (**F**) Representative dot plot and the quantitation of intracellular staining of T-bet in purified CD8$^+$ T cells after α-CD3/α-CD28 stimulation for 72 h. At least four mice were included in each group. Data in the bar graphs are represented as mean ± SEM. Statistical analysis used Student *t* test (ns, $p > 0.05$, *$p < 0.05$, **$p < 0.01$, ***$p < 0.001$, ****$p < 0.0001$).

which was consistent with our previous report that NOD-*Ncf1*^{m1J} CD4$^+$ T cells have decreased Th1 responses (13). TNF-α and granzyme B were also reduced in the NOD-*Ncf1*^{m1J} CD8$^+$ T cells after α-CD3 and α-CD28 stimulation (Fig. 1A). Similarly, effector molecules were reduced in B6-*Ncf1*^{m1J} CD8$^+$ T cells. The percentage of cells positive for the transcription factor T-bet (45.1 ± 1.2 [B6, $n = 8$] versus 33.9 ± 1.0 [B6-*Ncf1*^{m1J}, $n = 7$]; $p < 0.0001$) as well as IFN-γ (52.7 ± 2.9 [B6] versus 41.1 ± 0.8 [B6-*Ncf1*^{m1J}]; $p = 0.003$) and granzyme B (54.6 ± 4.6 [B6] versus 30.9 ± 3.4 [B6-*Ncf1*^{m1J}]; $p = 0.002$) were all significantly reduced in B6-*Ncf1*^{m1J} CD8$^+$ T cells. In addition, quantitative real-time PCR was carried out with α-CD3/α-CD28–stimulated CD8$^+$ T cells. IFN-γ and granzyme B transcripts were significantly reduced in NOD-*Ncf1*^{m1J} CD8$^+$ T cells (Fig. 1B). No significant differences between NOD and NOD-*Ncf1*^{m1J} CD8$^+$ T cells were observed in the mRNA levels of *Tnf*, *Il2*, *Fasl*, or *Prf1* (Fig. 1B). In addition, no changes were observed in *Lamp1*, *Il4*, *Il10*, *Il17*, or *Tfgb1* (not shown). This indicated that a functional NOX2 is essential for the production of specific proinflammatory cytokines (IFN-γ) and specific cytotoxic molecules (granzyme B). In accordance with similar *Il2* transcription (Fig. 1B), activation-induced CD8$^+$ T cell proliferation from the two strains was indistinguishable (Fig. 1C). Apoptosis (Fig. 1D) was equal in cells with and without NOX2 activity. A difference in activation status, measured as CD8$^+$ CD62L$^-$CD69$^+$ cells, was observed when comparing α-CD3– and α-CD28–stimulated NOD and NOD-*Ncf1*^{m1J} CD8$^+$ T cells at 24 h; however, this difference was not present 48 or 72 h after activation (Fig. 1E). These data indicate that the loss of ROS production in CD8$^+$ T cells resulted in a selective deficiency in a Tc1 effector phenotype in both the NOD and B6 genetic backgrounds.

To define the mechanism behind the selective loss of IFN-γ and granzyme B, we sought to investigate the canonical transcription factor of the Tc1 cell lineage, T-bet (41–43). Intracellular staining showed that T-bet levels were decreased in activated NOD-*Ncf1*^{m1J} CD8$^+$ T cells compared with wild-type controls (Fig. 1F). The other transcriptional factor related to IFN-γ and granzyme B production, Eomes (41), was present at equal levels in activated NOD and NOD-*Ncf1*^{m1J} CD8$^+$ T cells (not shown). These results suggest that ROS potentiates T-bet expression to promote CD8$^+$ T cell effector function.

The NOX2 inhibitor, apocynin, suppresses the production of effector molecules in mouse CD8$^+$ T cells

Production of ROS by NOX2 can be suppressed by apocynin, a specific inhibitor of p47^{phox}, the gene product of *Ncf1* or *NCF1* (44). Apocynin did not alter CD8$^+$ T cell viability (Supplemental Fig. 2A) or proliferation (Fig. 2D and Supplemental Fig. 2B), but it did inhibit IFN-γ production in a dose-dependent manner (Supplemental Fig. 2C), with 200 μM exhibiting maximal effects. To confirm the role of NOX2 in CD8$^+$ T cell effector function, splenic CD8$^+$ T cells were stimulated for 72 h with plate-bound α-CD3 and α-CD28 in the presence or absence of 200 μM apocynin. Consistent

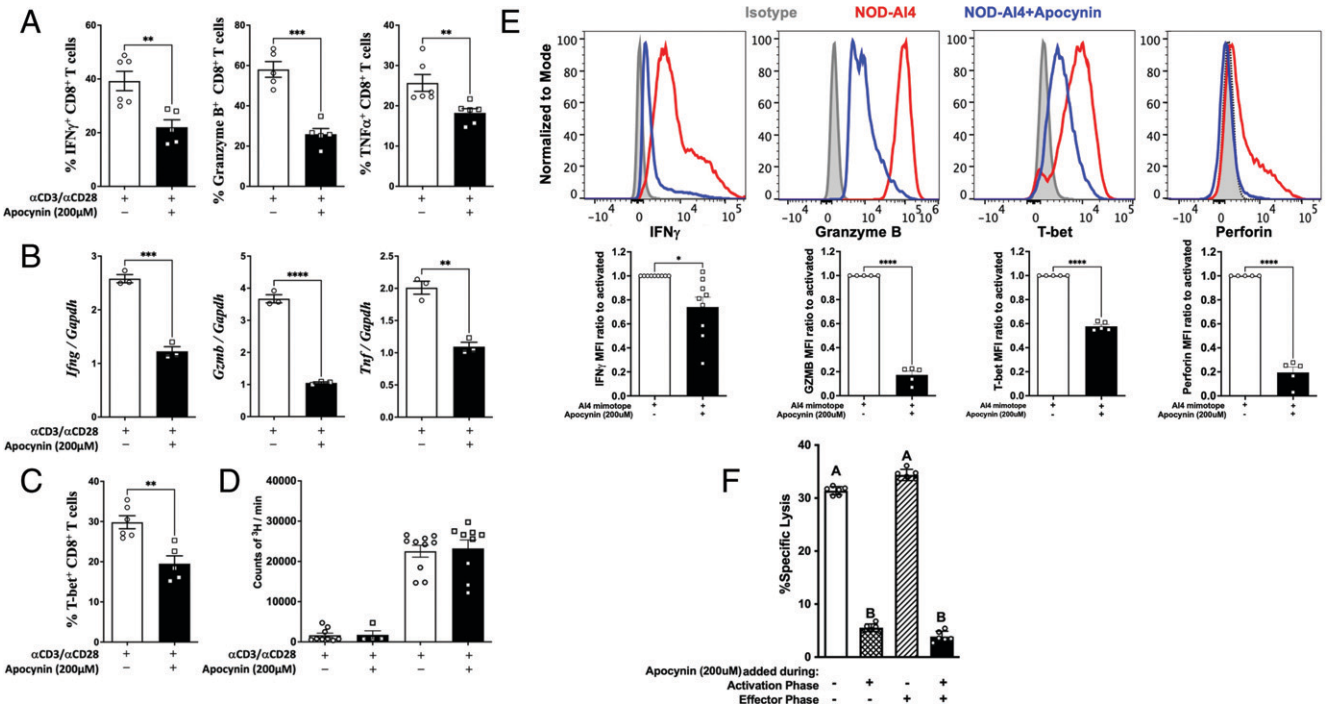

FIGURE 2. NOX2 is essential for effector function and cytolytic activity of $CD8^+$ T cells. (**A**–**D**) $CD8^+$ T cells from NOD spleens were activated with plate-bound α-CD3/α-CD28 with or without the presence of apocynin 200 μM. (A) Quantitation of intracellular staining for IFN-γ, granzyme B, and TNF-α. (B) Real-time quantitative PCR for IFN-γ, granzyme B, and TNF-α. cDNA was pooled from at least three mice, and the results represent three independent experiments done in triplicate. (C) Quantitation of intracellular staining of T-bet in NOD $CD8^+$ T cells. (D) Proliferation of NOD $CD8^+$ T cells. (**E**) Intracellular staining and quantitative analysis of IFN-γ, granzyme B, T-bet, and perforin expression in autoreactive monoclonal AI4 $CD8^+$ T cells after stimulation by specific mimotope for 72 h either without (open bars) or with (black bars) apocynin (200 μM). Gated on Live/Dead_NIR$^-$CD3$^+$CD8$^+$ cells. (**F**) AI4-induced CML is significantly reduced when NOX2 was inhibited during T cell activation but not during the effector phase. AI4 T cells were activated by Ag with [$CD8^+$ T cell activation phase (+)] or without [$CD8^+$ T cell activation phase (−)] apocynin. ^{51}Cr-labeled NIT-1 NOD-derived β cells were seeded in 96-well culture plates and cultured with preactivated AI4 cells at an E:T ratio of 20:1 for 16 h with apocynin [effector phase (+)] or without apocynin [effector phase (−)]. Data in the bar graphs are represented as mean ± SEM. Statistical analysis used Student *t* test (*$p < 0.05$, **$p < 0.01$, ***$p < 0.001$, **** $p < 0.0001$). In (F), for variables with a different letter, the difference is statistically significant at a level ≤0.05, whereas bars with the same letter are not statistically different (using one-way ANOVA).

with the observations in NOD-*Ncf1*^{m1J}, apocynin dramatically suppressed production of granzyme B, IFN-γ, and TNF-α protein levels (Fig. 2A) and corresponding mRNA transcripts (Fig. 2B). Apocynin-treated NOD $CD8^+$ T cells showed a 30% reduction in intracellular T-bet after α-CD3 and α-CD28 stimulation (Fig. 2C), which was similar to results with NOD-*Ncf1*^{m1J} $CD8^+$ T cells (Fig. 1F).

To confirm that NOX2 activity during $CD8^+$ T cell activation was not restricted to the autoimmune-prone NOD mouse, purified splenic $CD8^+$ T cells from C57BL/6 (B6) mice were stimulated with α-CD3 and α-CD28 with or without apocynin. T-bet, IFN-γ, and granzyme B were assessed by intracellular staining. The percentage of cells positive for the transcription factor T-bet (40.9 ± 2 [B6] versus 18.8 ± 2.1 [B6 + apocynin]; $p < 0.0001$) as well as IFN-γ (49.2 ± 4.4 [B6] versus 28.9 ± 1.9 [B6 + apocynin]; $p = 0.0027$) and granzyme B (50.3 ± 6.6 [B6] versus 23.2 ± 3.7 [B6 + apocynin]; $p = 0.0027$; $n = 5$ for each) were all reduced in B6 $CD8^+$ T cells when activated in the presence of apocynin. This phenotype was similar to what was observed in NOD $CD8^+$ T cells (Figs. 1 and 2). Similarly, B6 cells treated with and without apocynin had comparable upregulation of CD69 and similar levels of proliferation.

Inhibition of NOX2 blocks cytolytic capacity during Ag-specific activation of CD8$^+$ T cells

To determine how the loss of NOX2-derived ROS production impacts Ag-specific $CD8^+$ T cell activation, we used $CD8^+$ T cells from the highly pathogenic AI4 TCR-transgenic NOD mouse (NOD.AI4α/β-*Rag1*$^{-/-}$) (36). Upon Ag-specific activation of AI4 cells, a stark reduction in the intracellular staining of IFN-γ, granzyme B, T-bet, and perforin occurred when NOX2 was inhibited by apocynin (Fig. 2E).

An intact *Ncf1* in $CD8^+$ T cells was critical for efficient adoptive transfer of T1D (8), and the loss of NOX2 activity resulted in reduced $CD8^+$ T cell cytokine and effector molecule production (Figs. 1 and 2). Thus, we hypothesized that NOX2 activity is essential for cytolytic activity of $CD8^+$ T cells. AI4 effector cells were activated by the specific mimotope for 72 h (activation phase) prior to use in the CML assay (effector phase) using the NOD-derived NIT-1 pancreatic β-cell line as a target (36). As expected, AI4 cells that were not exposed to apocynin during either the activation or effector phase effectively lysed NIT-1 cells (Fig. 2F, first bar). β-Cell killing was prevented when AI4 T cells were treated with apocynin during only the activation phase (Fig. 2F, second bar). In stark contrast, the addition of apocynin during only the CML assay did not affect cytotoxic capability (Fig. 2F, third bar). Finally, apocynin treatment of AI4 T cells during both phases significantly reduced lysis. NOX2 is vital for diabetogenic T cell–mediated β-cell killing, and oxidants produced by this enzyme are important during activation/differentiation and likely involved in proximal TCR signaling.

NOX2 regulates T-bet, IFN-γ, granzyme B, and effector function of human CD8$^+$ T cells

Similar to mouse CD8$^+$ T cells, apocynin reduced IFN-γ production from human CD8$^+$ T cells in a dose-dependent manner (Supplemental Fig. 2D). The inhibition of NOX2 in human CD8$^+$ T cells with 200 μM apocynin led to a significant increase in proliferation (Fig. 3A). Whereas proliferation was enhanced in the presence of apocynin, inhibition of NOX2 by apocynin during α-CD3 and α-CD28 activation blunted production of IFN-γ, granzyme B, and T-bet (Fig. 3B–3D), similar to results with CD8$^+$ T cells from NOD and B6 mice. An in vitro model of Ag-specific target cell killing was used to determine the impact of NOX2 inhibition on CD8$^+$ cytolytic function (Fig. 3E). When apocynin (200 μM) was absent from both the activation and effector phases, the CTL efficiently lysed the BL5 cells (Fig. 3E, open bar). However, when apocynin was added during the activation phase, lysis of BL5 cells fell to less than 10% (Fig. 3E, checkered bar). Inhibition of NOX2 during only the effector phase led to a mild reduction in lysis (Fig. 3E, hatched bar). Apocynin during both the activation and effector phases resulted in an almost complete inhibition of lysis (Fig. 3E, filled bar), comparable to that observed when NOX2 was inhibited during the activation phase alone. These results are similar to the observations using mouse CD8$^+$ T cells, where inhibition of NOX2 during CD8$^+$ T cell activation led to a reduction in T-bet and effector cytokines/molecules with almost complete ablation of cytolytic activity without blunting proliferation. Therefore, NOX2 activity is essential for human and mouse CD8$^+$ T cell effector function.

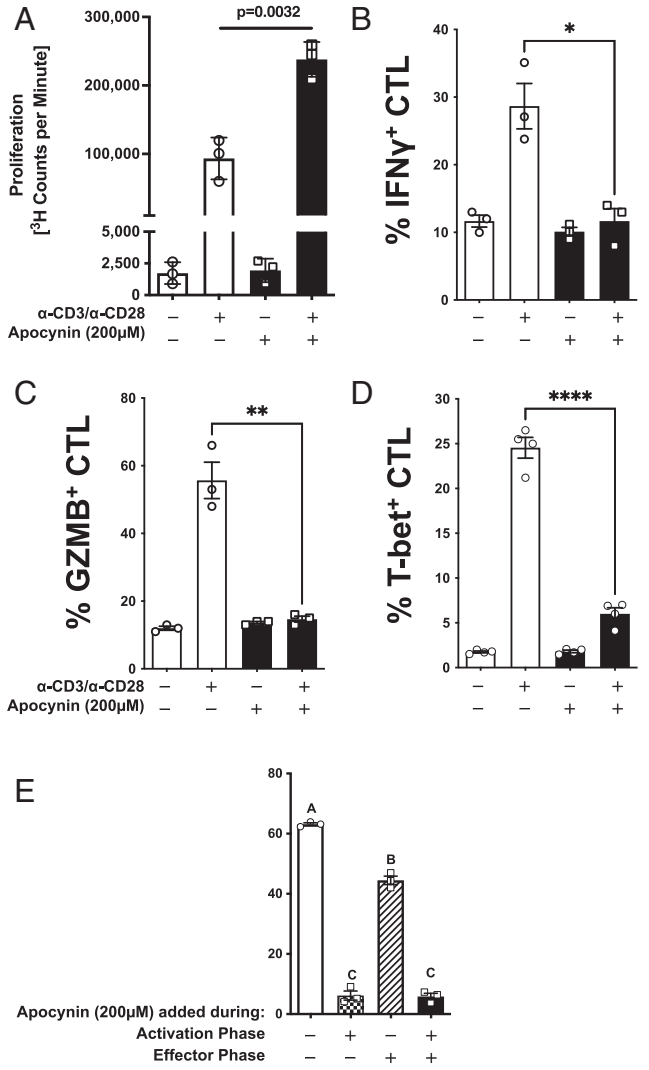

FIGURE 3. NOX2 is essential for effector function of human CD8$^+$ T cells. Purified naive CD8$^+$ T cells from three healthy volunteers were activated with α-CD3 and α-CD28 in the presence (black) or absence (open) of 200 μM apocynin. (**A**) Proliferation was assessed by ^{3}H-TdR incorporation at 72 h. Quantitation of intracellular staining for (**B**) IFN-γ, (**C**) granzyme B, and (**D**) T-bet in purified CD8$^+$ T cells (5×10^5 cells) after α-CD3 and α-CD28 stimulation for 72 h with (black) or without (open) 200 μM apocynin. (**E**) Purified naive human CD8$^+$ T cells from three donors were activated in the presence or absence of 200 μM apocynin for 48 h, transduced with a lentivirus encoding an IGRP-TCR, and then expanded for an additional 7 d in IL-2 (20 U/ml) with α-CD3/α-CD28 Dynabeads. Apocynin (200 μM) was present in specific cultures during the entire CD8$^+$ T cell activation phase (activation phase +). Additionally, CD8$^+$ T cells were activated in the absence of apocynin (activation phase −). The CD8$^+$ T cell effector phase was performed by coculturing IGRP reactive CD8$^+$ T cells with BL-5 at an E:T ratio of 25:1 with 200 μM apocynin (effector phase +) or without (effector phase −). Data are represented as mean ± SEM. For (A)–(E), statistical analysis used Student *t* test (*$p < 0.5$, **$p < 0.01$, ****$p < 0.0001$). In (E), bars with different letters were statistically different at a level $p < 0.05$, and, likewise, bars with the same letter were not statistically different (using one-way ANOVA).

H_2O_2, but not superoxide, promotes CD8$^+$ T cell function

NOX2 produces superoxide as a direct product (9). In vivo, superoxide is dismutated to H_2O_2 by SOD family members. H_2O_2 can subsequently be catalyzed into H_2O by catalase (45, 46). Superoxide can travel through the membrane via chloride voltage-gated channel 3 (ClC-3), and H_2O_2 crosses the membrane into the cytosol via aquaporin or diffusion (6, 47). The type of oxidant that modulates the effect of NOX2 in CD8$^+$ T cells was examined. Purified NOD CD8$^+$ T cells were treated with or without SOD1 and stimulated with α-CD3– and α-CD28–conjugated beads. SOD1 had little impact on the synthesis or secretion of IFN-γ (Fig. 4A, 4B). In addition, SOD1 had no effect on the synthesis of granzyme B or TNF-α (Fig. 4A). Accordingly, SOD1 treatment had no effect on T-bet (Fig. 4C).

To examine the effect of H_2O_2, purified NOD CD8$^+$ T cells were treated with or without catalase and stimulated with α-CD3 and α-CD28. Catalase treatment significantly suppressed production of IFN-γ, granzyme B, and TNF-α (Fig. 4A, 4B). Furthermore, T-bet expression after α-CD3 and α-CD28 stimulation also was significantly reduced following catalase treatment (Fig. 4C). Therefore, H_2O_2 transmits the redox signal to promote T-bet expression and effector function in CD8$^+$ T cells. Interestingly, unlike NOD-*Ncf1*^{m1J} or apocynin-treated cells, CD8$^+$ T cell proliferation was dramatically suppressed by scavenging H_2O_2 (Fig. 4D). This is consistent with a role for a NOX2-independent ROS source, such as mitochondrial ROS, in IL-2 production and CD8$^+$ T cell proliferation (48). Indeed, addition of IL-2 to the catalase-treated CD8$^+$ T cells partially rescued cell proliferation (Fig. 4D).

To determine if the defective effector functions associated with loss of NOX2 activity persist when proximal signaling events are bypassed, NOD and NOD-*Ncf1*^{m1J} CD8$^+$ T cells were activated with PMA and ionomycin (49). When NOD-*Ncf1*^{m1J} CD8$^+$ T cells were activated by PMA and ionomycin, protein levels of IFN-γ, granzyme B, and T-bet were equal to NOX2-intact NOD CD8$^+$ T cells (Supplemental Fig. 3A). Similarly, catalase treatment did not impact CD8$^+$ T cells activated with PMA/ionomycin (Supplemental Fig. 3B). Therefore, NOX2-derived H_2O_2 acts proximally but not distally in TCR signaling.

NOX2 activity impacts TCR signaling at the TSC1/2 complex to promote mTORc1 activity

Proximal TCR signaling events include activation of AKT by PI3K and subsequent repression of the TSC1/2 complex (40). The inactivation of TSC1/2 results in elevated RheB-GTP levels that

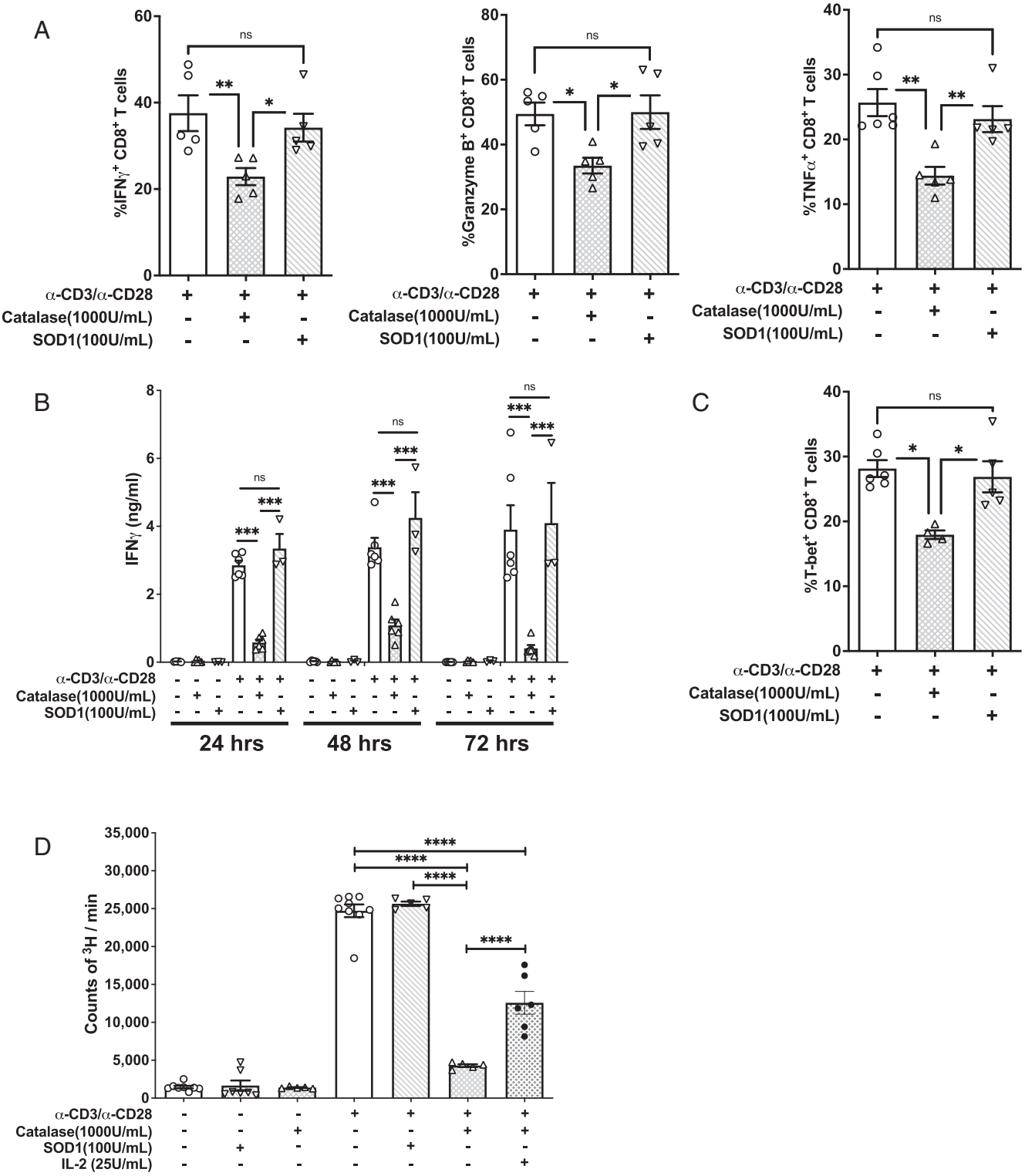

FIGURE 4. Hydrogen peroxide scavenging significantly blunts $CD8^+$ T cell effector function after α-CD3/α-CD28 stimulation. NOD $CD8^+$ T cells were stimulated by α-CD3/α-CD28 for 3 d in the presence or absence of catalase or SOD1. (**A**) Intracellular levels of IFN-γ, granzyme B, and TNF-α were assessed. (**B**) IFN-γ was measured by ELISA on days 1, 2, and 3. (**C**) Intracellular staining for T-bet in $CD8^+$ T cells. (**D**) $CD8^+$ T cell proliferation was assessed by [^{3}H]TdR incorporation. Results are presented as mean ± SEM. Each measure was compiled from four independent observations performed in triplicate. (*$p < 0.05$, **$p < 0.01$, ***$p < 0.001$, ****$p < 0.0001$).

can promote mTORc1 activity leading to downstream effects on T-bet, IFN-γ, and granzyme B (5). The AKT pathway was not altered, because lysates of α-CD3– and α-CD28–stimulated NOD and NOD-*Ncf1*^{m1J} $CD8^+$ T cells displayed comparable p-GSK levels (Fig. 5A). However, differences in TSC1/2 activity were observed, because RheB-GTP significantly increased after activation of NOD $CD8^+$ T cells, whereas an increase in RheB-GTP was not observed in NOD-*Ncf1*^{m1J} cells (Fig. 5B). Total RheB levels were not different when we compared unactivated or activated $CD8^+$ T cells from either strain.

mTORc1 is essential for $CD8^+$ T cell effector function through promoting T-bet expression (5). In fibroblasts, mTORc1 activity can

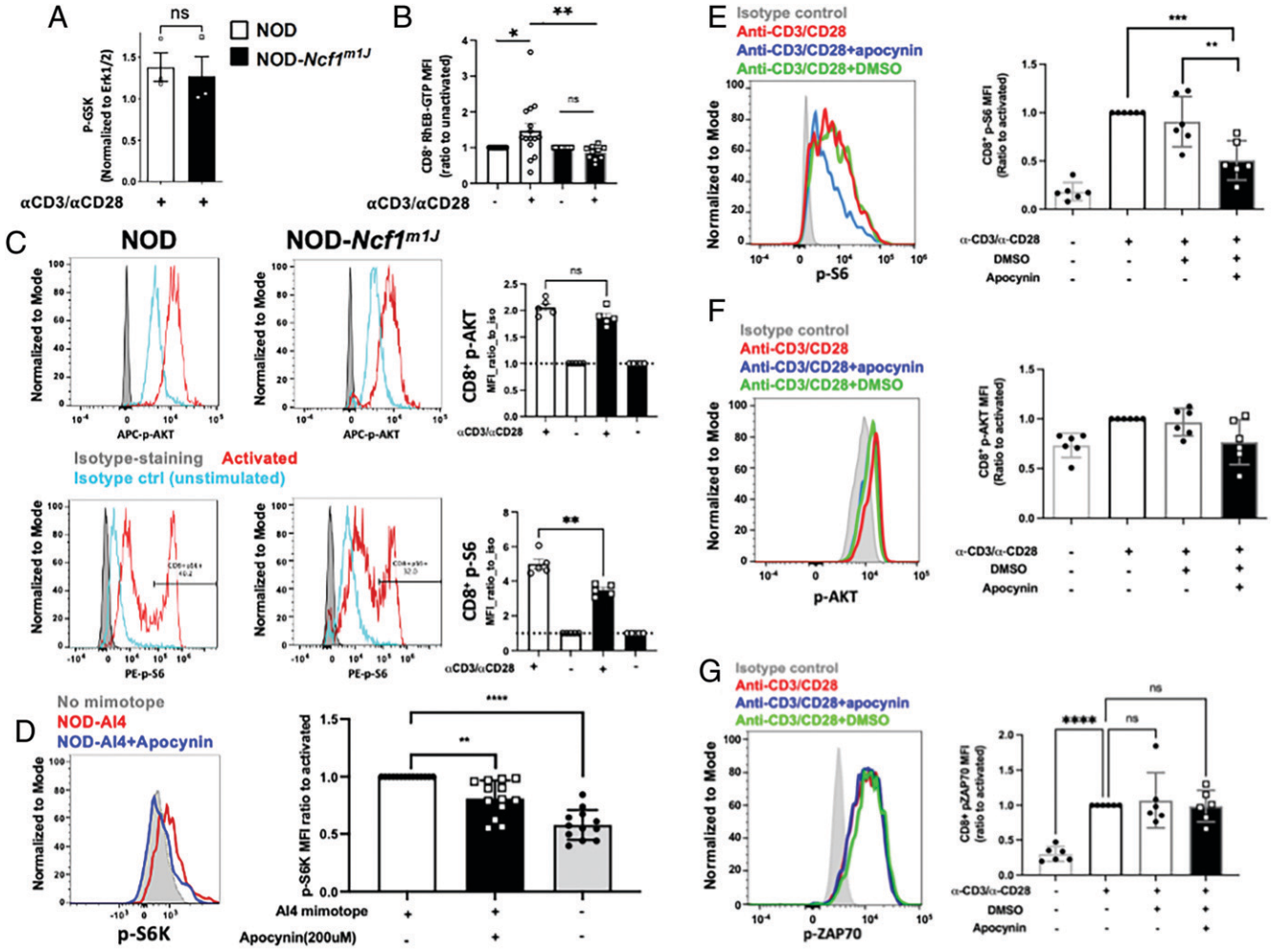

FIGURE 5. NOX2 activity is required for TSC1/2 repression and downstream mTORc1 activation during $CD8^+$ T cell activation. (**A**) NOD or NOD-*Ncf1*^{m1J} $CD8^+$ T cells were activated by α-CD3/α-CD28 for 30 min and subjected to immunoprecipitation of p-GSK. Cellular p-GSK levels, a marker of Akt kinase activity, were determined relative to the input control Erk1/2. (**B**) NOD or NOD-*Ncf1*^{m1J} splenocytes were activated by α-CD3/α-CD28 for 10 min and subjected to flow cytometry. Intracellular levels of RheB-GTP were determined by staining with Abs and analyzed in $LDY^-CD3^+CD8^+$ population. (**C**) Splenocytes from NOD (open bars) and NOD-*Ncf1*^{m1J} (black bars) were stimulated with soluble α-CD3/α-CD28 or isotype hamster IgG controls for 30 min with protein G as a crosslinker. Surface T cell markers together with p-AKT and p-S6 were detected using flow cytometry. Representative histograms of NOD (left) and NOD-*Ncf1*^{m1J} were shown, gated on Live/Dead_$NIR^-CD3^+CD8^+$. Data are expressed as MFI ratio to isotype control (unstimulated, blue histogram); $n = 5$ each. (**D**) Intracellular staining and quantitative analysis of pS6K in autoreactive monoclonal AI4 $CD8^+$ T cells after stimulation by specific mimotope for 30 min either without (open bars) or with (black bars) apocynin (200 μM). Gated on Live/Dead_$NIR^-CD3^+CD8^+$. (**E–G**) Human PBMCs from healthy donors ($n = 6$) with or without pretreatment of apocynin (400 μM) were activated with α-CD3/α-CD28 for 10 min. Surface markers and intracellular p-S6, p-AKT, and p-ZAP70 were stained with fluorescent Abs and detected using a flow cytometer. Shown are p-S6 (E), p-AKT (F), and p-ZAP70 (G) MFI ratio to activated (the second group), gated on Live/Dead-$Yellow^-CD3^+CD8^+$ T cells. Results are compared using Student *t* test or one-way ANOVA multiple comparisons (**$p < 0.01$, ***$p < 0.001$, ****$p < 0.0001$).

be promoted by oxidants through a process that is dependent on oxidation and repression of TSC1/2 function (50). We therefore hypothesized that NOX2-derived ROS may enhance $CD8^+$ T cell effector function by promoting mTORc1, an upstream mediator of T-bet. mTORc1 phosphorylates S6K at T389 (p-S6K). p-S6K further phosphorylates S6. Both p-S6K and p-S6 can be used as indicators of mTORc1 activity (50, 51). In vitro activation of splenocytes from NOD mice exhibited a significant increase in p-S6 in $CD8^+$ T cells, indicating sufficient mTORc1 activity upon TCR stimulation. Meanwhile, S6 phosphorylation was significantly lower in activated NOD-*Ncf1*^{m1J} $CD8^+$ T cells, whereas p-AKT levels were similar (Fig. 5C). This was further confirmed through inhibition of NOX2 by apocynin leading to lower p-S6K in Ag-specific activation of mouse AI4 $CD8^+$ T cells (Fig. 5D). In addition, we were able to show the same effect of apocynin in human $CD8^+$ T cells. Lack of NOX2 function inhibited activation-induced p-S6 (Fig. 5E) but not p-AKT (Fig. 5F) or p-ZAP70 (Fig. 5G) in human $CD8^+$ T cells. These data support the hypothesis that a functional NOX2 inactivates TSC1/2, resulting in downstream TCR-dependent Rheb-GTP and mTORc1 activation in $CD8^+$ T cells.

To confirm that mTORc1 was required for $CD8^+$ T cell effector function, we treated $CD8^+$ T cells with the mTORc1 inhibitor rapamycin and activated the cells with α-CD3 and α-CD28. Inhibition of mTORc1 dramatically reduced IFN-γ, granzyme B, and TNF-α production in $CD8^+$ T cells (Fig. 6A). Suppression was observed as early as 24 h after stimulation, indicating that inhibition of mTORc1 interrupts early events during $CD8^+$ T cell activation (Fig. 6B). Consistent with a previous report (5), the compromised effector function results from a reduction in T-bet production after activation of rapamycin-treated $CD8^+$ T cells (Fig. 6C).

Redox regulation of mTORc1 activity in $CD8^+$ T cells

The compromised mTORc1 activity in NOD-*Ncf1*^{m1J} (Fig. 5C) led us to propose that mTORc1 activity in NOD $CD8^+$ T cells is redox

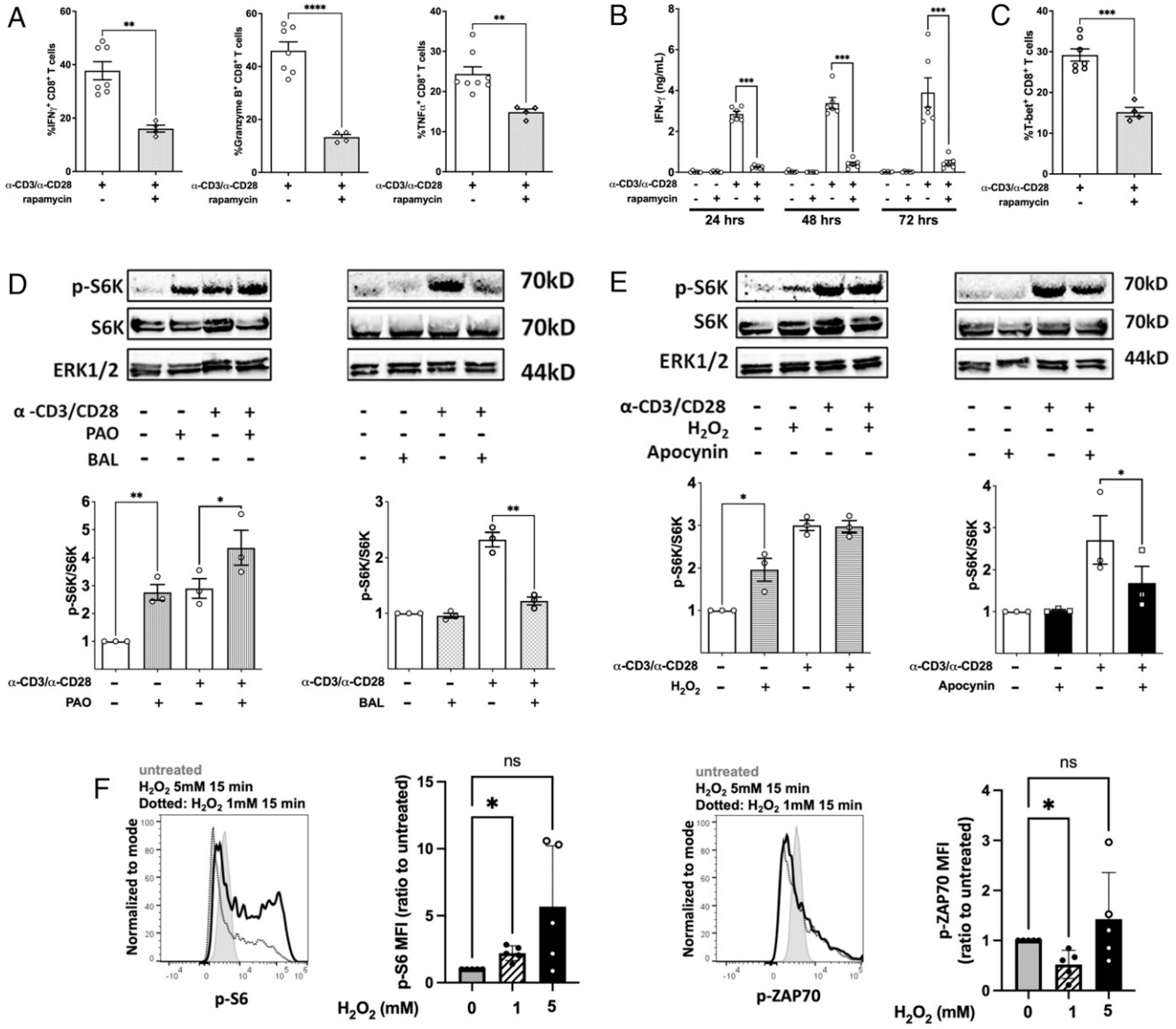

FIGURE 6. mTORc is required for CD8$^+$ T cell effector function through promoting transcriptional activity of T-bet through a redox-regulated mechanism. (**A**) Flow cytometry quantitation of intracellular staining of the IFN-γ, granzyme B, and TNF-α in purified NOD CD8$^+$ T cells stimulated by α-CD3/α-CD28 for 66 h in the presence or absence of 20 ng/ml rapamycin followed by restimulation with PMA/ionomycin plus GolgiStop for 6 h. (**B**) NOD CD8$^+$ T cells (5×10^4) were stimulated by α-CD3/α-CD28 in the presence or absence of 20 ng/ml rapamycin. IFN-γ was measured by ELISA on days 1, 2, and 3. (**C**) Intracellular staining for T-bet in CD8$^+$ T cells after a 72-h polyclonal stimulation. NOD CD8$^+$ T cells were treated with (**D**) PAO or BAL or (**E**) H_2O_2 or apocynin either with or without activation by α-CD3/α-CD28 for 30 min. Phosphorylation of S6K was measured by the ratio of phosphorylated S6K and total SK6. Results are from three independent experiments. Untreated NOD CD8$^+$ T cells were used as the reference group for normalization among multiple tests. (**F**) H_2O_2 slightly increased p-S6 but not p-ZAP70 in human CD8$^+$ T cells. Human PBMCs were treated with H_2O_2 at the indicated concentrations for 15 min at 37°C, and p-S6 and p-ZAP70 were stained with fluorescent Abs and detected with a flow cytometer. Shown are MFI ratio to untreated (first group). Gated on Live/Dead-Yellow$^-$CD3$^+$CD8$^+$ T cells. Results are presented as mean ± SEM. Student *t* test was performed to exclude potential batch effects (*$p < 0.05$, **$p < 0.01$, ***$p < 0.001$, ****$p < 0.0001$).

dependent. To explore this possibility, the effect of oxidants or antioxidants upon mTORc1 activation was assessed. PAO is a cell-permeable reagent that crosslinks vicinal thiol groups and thus was used as a cysteine oxidant. BAL was used as a reducing reagent. According to previous reports, PAO is able to significantly promote the phosphorylation of S6K by mTORc1 in HEK293T cells, whereas BAL blocks the PAO-induced or endogenous oxidant-mediated mTORc1 activation in these cells (50, 52). NOD CD8$^+$ T cells were treated with either PAO or BAL in the presence or absence of α-CD3 and α-CD28 for 45 min. In the absence of TCR activation, phosphorylation of S6K was increased by PAO (Fig. 6D). When CD8$^+$ T cells were treated with BAL, p-S6K was dramatically decreased to basal levels even in the presence of α-CD3 and α-CD28 stimulation (Fig. 6D). This confirmed the positive effect of oxidants on mTORc1 in CD8$^+$ T cells. Because our data demonstrate that H_2O_2 could be the effector molecule of NOX2 to elicit the redox signal in T cell activation, we tested the ability of H_2O_2 to promote mTORc1 activity in CD8$^+$ T cells. NOD CD8$^+$ T cells were treated with 10 μM H_2O_2 and then activated with α-CD3 and α-CD28. Similar to the PAO treatment of resting CD8$^+$ T cells, H_2O_2 promoted phosphorylation of S6K even in the absence of polyclonal stimulation. However, such a low dose of H_2O_2 did not potentiate mTORc1 activity during polyclonal activation of T cells. A plausible explanation was that this resulted from redundant

ROS produced in NOX2-intact CD8$^+$ T cells after TCR engagement (Fig. 6E). To confirm NOX2 as the H_2O_2 source, CD8$^+$ T cells were treated with apocynin, and S6K phosphorylation was assessed with or without α-CD3 and α-CD28 stimulation. Consistent with NOD-*Ncf1*^{m1J} CD8$^+$ T cells, when NOX2-intact CD8$^+$ T cells were activated in the presence of apocynin, p-S6K levels were significantly reduced (Fig. 6E). The effect of H_2O_2 was confirmed in human PBMCs. As shown in Fig. 6F, PBMCs were treated with either 1 mM or 5 mM H_2O_2 for 15 min at 37°C. Flow cytometric analysis revealed that H_2O_2 treatment slightly but significantly induced CD8$^+$ T cell p-S6 but not p-ZAP70 that is proximal to the TCR. Taken together, these data demonstrate that NOX2-derived H_2O_2 by CD8$^+$ T cells can mediate TCR signaling through mTORc1 via TSC1/2, as shown in our proposed model (Fig. 7).

Discussion

During the interaction of naive T cells with APCs, TCR signaling is coordinated with secondary and tertiary signals to decide T cell fate and differentiation (53). Previous studies have demonstrated that ROS govern processes of T cell activation, including IL-2 production, proliferation, differentiation, and effector function (7, 13, 39, 54–56). In T cells, various ROS generators collaboratively promote cell activation and govern effector phenotypes (48, 55). In the present study, we have identified that another ROS generator, NOX2, is vital for CD8$^+$ T cell activation by promoting effector function and cytotoxicity through the mTORC1–T-bet axis signaling pathway (Fig. 7).

T1D is mediated primarily by autoreactive T cell responses. Both clinical and basic science reports have provided evidence that supports a role for ROS in the pathogenesis of T1D (57). CD8$^+$ T cells are recognized as a major effector cell type in mediating β-cell death in T1D (24, 58, 59). Multiple reports suggest that the transcriptional factor T-bet is required in the development of T1D by promoting CTL effector differentiation (60–62). Our previous studies have indicated that NOX2 promotes Th1 differentiation via T-bet in NOD CD4$^+$ T cells (13) and is required for full effector function of CD8$^+$ T cells in T1D using both NOD-*Ncf1*^{m1J} and adoptive transfer models. In the present study, to our knowledge, we have discovered a novel mechanism whereby NOX2-derived ROS promotes CTL effector function through enhancing T-bet expression. Stimulated NOD-*Ncf1*^{m1J} CD8$^+$ T cells showed a reduction in T-bet expression and suppression of CD8$^+$ T cell effector responses, including IFN-γ, granzyme B, and TNF-α production. Similarly, when treated with the NOX2 inhibitor apocynin, polyclonal activation of CD8$^+$ T cells from the NOD and B6 strains showed a decline in T-bet synthesis (Fig. 2). These results were extended to human model systems where inhibition of NOX2 during activation prevents T-bet, IFN-γ, and granzyme B expression and effector function of both human and mouse CD8$^+$ T cells (Fig. 3). CD8$^+$ T cell proliferation was not impacted when NOX2 was inactive due to genetic ablation or pharmacological inhibition, which is consistent with a previous report on the proliferative capacity of T-bet knockout CD8$^+$ T cells (61).

The treatment of diabetogenic AI4 CD8$^+$ T cells with apocynin during Ag-specific activation resulted in ablation of T-bet, IFN-γ, and granzyme B as well as β-cell cytolytic capability (Fig. 2). In contrast, if NOX2 was inhibited only during the CML assay, the lysis of β cells was equal to untreated AI4 CD8$^+$ T cells, suggesting that the effect of NOX2 is early during CD8$^+$ T cell activation and is not required for CD8$^+$ T cell degranulation. These results were confirmed in a human model E:T coculture system (Fig. 3). The fact that specific lysis of β cells was not impacted or only minimally affected by addition of apocynin during the effector phase of the

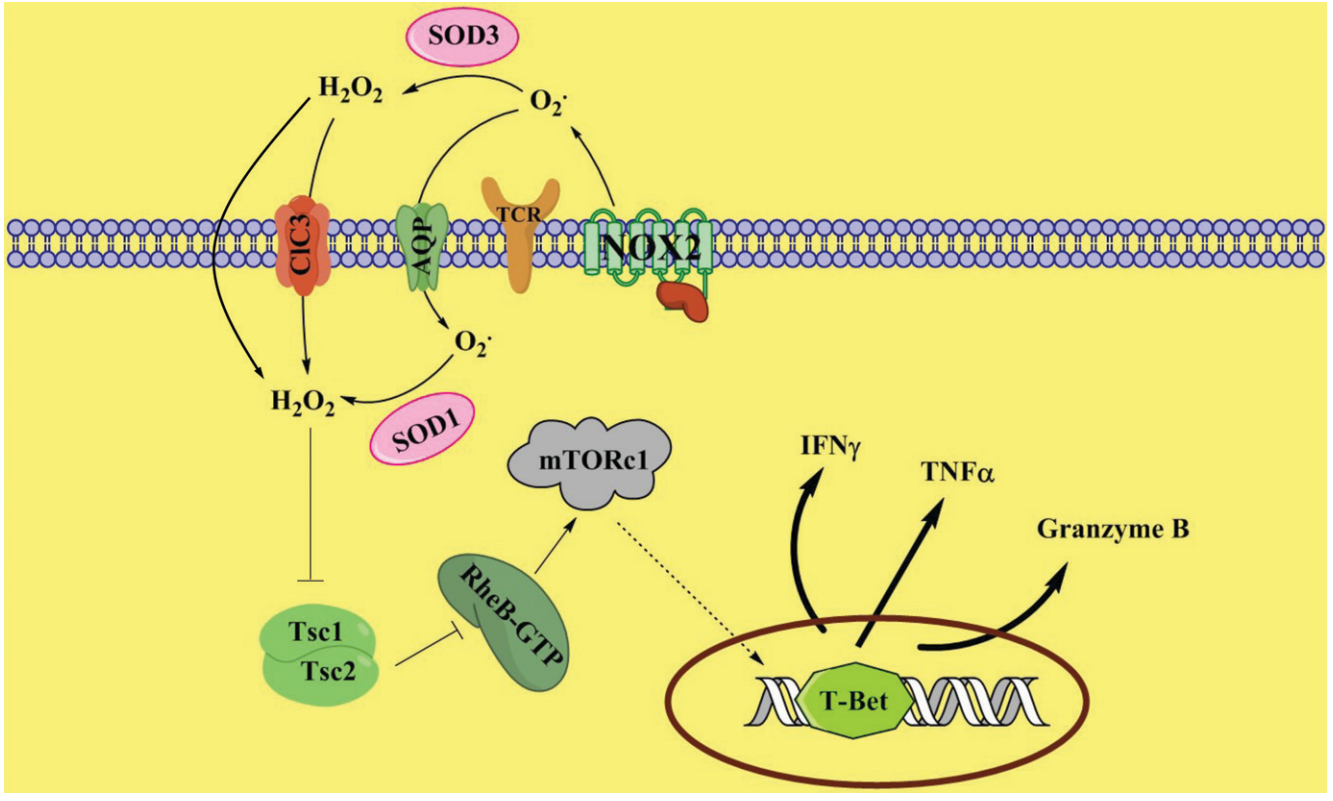

FIGURE 7. Proposed model of NOX2-mediated redox signaling during activation of CD8$^+$ T cells. Upon activation, NOX2 generates superoxide, which is dismutated into hydrogen peroxide, probably by superoxide dismutase. H_2O_2 in turn inhibits TSC1/2. Suppression of TSC1/2 activity promotes the levels of RheB-GTP, leading to enhanced mTORc1 activity. Upregulation of mTORc1 activity promotes T-bet expression and thus facilitates CD8$^+$ T cell effector function.

CML assay supports the notion that blocking NOX2 activity within the β cell would not provide significant protection of the β cells from lysis by $CD8^+$ T cells. The results corroborate our previous studies where NOD-*Ncf1*^{m1J} mice were susceptible to adoptive transfer of AI4 $CD8^+$ T cells (8). These data highlight an important role for NOX2 in promoting $CD8^+$ T cell effector function during the early events of activation.

Chronic granulomatous disease (CGD) is a primary phagocytic disorder in humans due to mutations in any subunits of the NADPH oxidase (NOX2 deficiency) leading to impaired ROS development and susceptibility to severe life-threatening infections (63). Exogenous IFN-γ has shown clinical benefit and is approved in the United States for the prevention of infections in CGD; however, its use remains controversial due to lack of a mechanism of action in CGD and variable clinical benefit (64, 65). These data may help to explain a possible mechanism of IFN-γ treatment in CGD (63, 64, 66–68). Exogenous IFN-γ acts on $CD8^+$ T cells to promote immunity against infections (69–71). Because IFN-γ or IL-12 can induce T-bet, administration or induction of innate immune cell production of these cytokines could enhance $CD8^+$ T cell function in response to infections (72–75) and as such could provide clinical benefit to patients with CGD.

NOX2 generates superoxide at the exterior side of the cell membrane (9, 10). Superoxide is thought to be transported across membranes by ClC-3, a member of the ClC voltage-gated chloride (Cl^-) channel superfamily. Alternatively, it could be converted into H_2O_2 outside of $CD8^+$ T cells that can then diffuse into the cytosol or be transported by aquaporins (47, 76, 77). Scavenging superoxide by treating $CD8^+$ T cells with SOD1 during polyclonal activation had little effect on proliferation or expression of T-bet, IFN-γ, granzyme B, or TNF-α; however, scavenging H_2O_2 resulted in significant decreases of these $CD8^+$ T cell effector molecules. This indicates that H_2O_2 instead of superoxide modulates $CD8^+$ T cell effector functions. $CD8^+$ T cell proliferation also was dramatically suppressed by catalase treatment, suggesting that a NOX2-independent source of ROS was functioning to promote $CD8^+$ T cell proliferation. Because mitochondrial ROS promotes T cell proliferation by enhancing IL-2 production (48), we conclude that in $CD8^+$ T cells, NOX2 and mitochondria-derived H_2O_2 enhance T cell activation by promoting effector differentiation and proliferation, respectively. Indeed, when IL-2 was added to the cultures during $CD8^+$ T cell activation with α-CD3/α-CD28 in the presence of catalase, proliferation was restored (Fig. 4D).

NOX2 promotes T-bet production through modulating mTORc1 activity after α-CD3 and α-CD28 stimulation of naive $CD8^+$ T cells. mTORc1 promotes the production of T-bet over its counterpart Eomes after $CD8^+$ T cell activation to regulate the balance between $CD8^+$ T cell effector and memory differentiation (5). Inhibition of mTORc1 with rapamycin had a dramatic suppressive effect on NOD $CD8^+$ T cell T-bet production, proinflammatory cytokines, and effector molecule expression, but with little impact on cell proliferation. $CD8^+$ T cells with *Ncf1* mutation or NOX2 inhibition were compromised in TCR-dependent mTORc1 activation. Our results provide data to add to a more complete picture of mTORc1 activation and induction of differentiation in $CD8^+$ T cells (78–82) to include NOX2-derived hydrogen peroxide as an upstream mediator of mTOR.

Hydrogen peroxide derived from NOX2 promotes CTL effector function. Hydrogen peroxide treatment of $CD8^+$ T cells activated mTORc1; however, when NOX2 produced enough free radicals upon α-CD3 and α-CD28 stimulation, H_2O_2 could not further promote mTORc1 activation. Treating NOD $CD8^+$ T cells with a cysteine-specific oxidant, PAO, greatly enhanced mTORc1 activity, even without the CD3/CD28 signal. In contrast, the antioxidant BAL inhibited the activation of this complex in $CD8^+$ T cells, confirming the significance of ROS in mTORc1 activation. mTORc1 activation is involved in multiple cellular pathways, and RheB-GTP, the active GTP bound form of RheB, is a major activator of mTORc1 by direct interaction (83, 84). In many cell types, RheB-GTP is negatively regulated by TSC1/2 by transforming RheB-GTP into RheB-GDP, the inactive form (85). Our data demonstrate that in the absence of NOX2-derived ROS, RheB-GTP levels are suppressed, indicating sustained TSC1/2 activity (Fig. 5B). Akt function was not impaired in the absence of NOX2, demonstrating that NOX2 regulates TSC1/2 activity in $CD8^+$ T cells in an Akt-independent manner as previously described using immortalized cell lines (50).

In summary, to our knowledge, this study provides a novel mechanism whereby oxidants regulate using $CD8^+$ T cell effector function. NOX2-derived H_2O_2 enhances RheB activity and thus promotes mTORc1 function during $CD8^+$ T cell activation, leading to an enhanced production of T-bet, which boosts the $CD8^+$ T cell effector function and cytolytic activity. The data reported in the present study do not support a global proinflammatory dysfunction in NOX-deficient animals. *Ncf1* mutations previously have been associated with increased severity of experimental allergic encephalomyelitis and collagen-induced arthritis (13, 86) but resistance to T1D (8, 13). Due to the essential role of $CD8^+$ T cells in T1D, NOX2-derived ROS play $CD8^+$ T cell extrinsic and intrinsic roles in pathogenesis. NOX2 promotes dendritic cell Ag cross-presentation and activation of naive $CD8^+$ T cells in T1D (extrinsic) (27), and, in the present study, we provide evidence for a $CD8^+$ T cell intrinsic role of NOX2 in regulating signal transduction leading to production of effector molecules and cytolytic function (Figs. 1–4 and 7). To our knowledge, our data provide new insights into potential targets for therapeutic strategies in organ transplantation or CTL-mediated autoimmune disease, such as T1D. In addition, due to the essential role of ROS in immune cell signal transduction, we predict that nontargeted antioxidant therapy or supplements might alter the thresholds for $CD8^+$ T cell effector function during immune responses.

Acknowledgments

The University of Florida Center for Immunology and Transplantation was essential to the completion of these studies.

Disclosures

The authors have no financial conflicts of interest.

References

1. Zhang, N., and M. J. Bevan. 2011. $CD8^+$ T cells: foot soldiers of the immune system. *Immunity* 35: 161–168.
2. Harty, J. T., A. R. Tvinnereim, and D. W. White. 2000. $CD8^+$ T cell effector mechanisms in resistance to infection. *Annu. Rev. Immunol.* 18: 275–308.
3. Araki, K., A. P. Turner, V. O. Shaffer, S. Gangappa, S. A. Keller, M. F. Bachmann, C. P. Larsen, and R. Ahmed. 2009. mTOR regulates memory CD8 T-cell differentiation. *Nature* 460: 108–112.
4. Mathieu, M., N. Cotta-Grand, J. F. Daudelin, P. Thébault, and N. Labrecque. 2013. Notch signaling regulates PD-1 expression during $CD8^+$ T-cell activation. *Immunol. Cell Biol.* 91: 82–88.
5. Rao, R. R., Q. Li, M. R. Gubbels Bupp, and P. A. Shrikant. 2012. Transcription factor Foxo1 represses T-bet-mediated effector functions and promotes memory $CD8^+$ T cell differentiation. *Immunity* 36: 374–387.
6. Winterbourn, C. C. 2008. Reconciling the chemistry and biology of reactive oxygen species. *Nat. Chem. Biol.* 4: 278–286.
7. Sklavos, M. M., H. M. Tse, and J. D. Piganelli. 2008. Redox modulation inhibits CD8 T cell effector function. *Free Radic. Biol. Med.* 45: 1477–1486.
8. Thayer, T. C., M. Delano, C. Liu, J. Chen, L. E. Padgett, H. M. Tse, M. Annamali, J. D. Piganelli, L. L. Moldawer, and C. E. Mathews. 2011. Superoxide production by macrophages and T cells is critical for the induction of autoreactivity and type 1 diabetes. *Diabetes* 60: 2144–2151.
9. Bedard, K., and K. H. Krause. 2007. The NOX family of ROS-generating NADPH oxidases: physiology and pathophysiology. *Physiol. Rev.* 87: 245–313.

10. Thamsen, M., and U. Jakob. 2011. The redoxome: proteomic analysis of cellular redox networks. *Curr. Opin. Chem. Biol.* 15: 113–119.
11. Panday, A., M. K. Sahoo, D. Osorio, and S. Batra. 2015. NADPH oxidases: an overview from structure to innate immunity-associated pathologies. *Cell. Mol. Immunol.* 12: 5–23.
12. El-Benna, J., P. M. Dang, M. A. Gougerot-Pocidalo, J. C. Marie, and F. Braut-Boucher. 2009. p47phox, the phagocyte NADPH oxidase/NOX2 organizer: structure, phosphorylation and implication in diseases. *Exp. Mol. Med.* 41: 217–225.
13. Tse, H. M., T. C. Thayer, C. Steele, C. M. Cuda, L. Morel, J. D. Piganelli, and C. E. Mathews. 2010. NADPH oxidase deficiency regulates Th lineage commitment and modulates autoimmunity. *J. Immunol.* 185: 5247–5258.
14. Horváth, R., D. Rožková, J. Lašťovička, A. Poloučková, P. Sedláček, A. Sedivá, and R. Spíšek. 2011. Expansion of T helper type 17 lymphocytes in patients with chronic granulomatous disease. *Clin. Exp. Immunol.* 166: 26–33.
15. Kuhns, D. B., W. G. Alvord, T. Heller, J. J. Feld, K. M. Pike, B. E. Marciano, G. Uzel, S. S. DeRavin, D. A. Priel, B. P. Soule, et al. 2010. Residual NADPH oxidase and survival in chronic granulomatous disease. *N. Engl. J. Med.* 363: 2600–2610.
16. Kuhns, D. B., A. P. Hsu, D. Sun, K. Lau, D. Fink, P. Griffith, D. W. Huang, D. A. L. Priel, L. Mendez, S. Kreuzburg, et al. 2019. *NCF1* ($p47^{phox}$)-deficient chronic granulomatous disease: comprehensive genetic and flow cytometric analysis. *Blood Adv.* 3: 136–147.
17. Chen, J., S. E. Stimpson, G. A. Fernandez-Bueno, and C. E. Mathews. 2018. Mitochondrial reactive oxygen species and type 1 diabetes. *Antioxid. Redox Signal.* 29: 1361–1372.
18. Daneman, D. 2006. Type 1 diabetes. *Lancet* 367: 847–858.
19. Newby, B. N., T. M. Brusko, B. Zou, M. A. Atkinson, M. Clare-Salzler, and C. E. Mathews. 2017. Type 1 Interferons potentiate human $CD8^+$ T-cell cytotoxicity through a STAT4- and granzyme B-dependent pathway. *Diabetes* 66: 3061–3071.
20. Newby, B. N., and C. E. Mathews. 2017. Type I interferon is a catastrophic feature of the diabetic islet microenvironment. *Front. Endocrinol. (Lausanne)* 8: 232.
21. Whitener, R. L., L. Gallo Knight, J. Li, S. Knapp, S. Zhang, M. Annamalai, V. M. Pliner, D. Fu, I. Radichev, C. Amatya, et al. 2017. The type 1 diabetes-resistance locus *Idd22* controls trafficking of autoreactive CTLs into the pancreatic islets of NOD mice. *J. Immunol.* 199: 3991–4000.
22. Anderson, M. S., and J. A. Bluestone. 2005. The NOD mouse: a model of immune dysregulation. *Annu. Rev. Immunol.* 23: 447–485.
23. Willcox, A., S. J. Richardson, A. J. Bone, A. K. Foulis, and N. G. Morgan. 2009. Analysis of islet inflammation in human type 1 diabetes. *Clin. Exp. Immunol.* 155: 173–181.
24. Tsai, S., A. Shameli, and P. Santamaria. 2008. $CD8^+$ T cells in type 1 diabetes. *Adv. Immunol.* 100: 79–124.
25. Lee, H. M., D. M. Shin, K. K. Kim, J. S. Lee, T. H. Paik, and E. K. Jo. 2009. Roles of reactive oxygen species in CXCL8 and CCL2 expression in response to the 30-kDa antigen of *Mycobacterium tuberculosis*. *J. Clin. Immunol.* 29: 46–56.
26. Roep, B. O. 2008. Islet autoreactive CD8 T-cells in type 1 diabetes: licensed to kill? *Diabetes* 57: 1156.
27. Liu, C., R. L. Whitener, A. Lin, Y. Xu, J. Chen, A. Savinov, J. W. Leiding, M. A. Wallet, and C. E. Mathews. 2019. Neutrophil cytosolic factor 1 in dendritic cells promotes autoreactive $CD8^+$ T cell activation via cross-presentation in type 1 diabetes. *Front. Immunol.* 10: 952.
28. Chen, J., and C. E. Mathews. 2014. Use of chemical probes to detect mitochondrial ROS by flow cytometry and spectrofluorometry. *Methods Enzymol.* 542: 223–241.
29. Li, Y., P. Y. Lee, E. S. Kellner, M. Paulus, J. Switanek, Y. Xu, H. Zhuang, E. S. Sobel, M. S. Segal, M. Satoh, and W. H. Reeves. 2010. Monocyte surface expression of Fcgamma receptor RI (CD64), a biomarker reflecting type-I interferon levels in systemic lupus erythematosus. *Arthritis Res. Ther.* 12: R90.
30. Zhuang, H., S. Han, Y. Xu, Y. Li, H. Wang, L. J. Yang, and W. H. Reeves. 2014. Toll-like receptor 7-stimulated tumor necrosis factor α causes bone marrow damage in systemic lupus erythematosus. *Arthritis Rheumatol.* 66: 140–151.
31. Chaparro, R. J., A. R. Burton, D. V. Serreze, D. A. Vignali, and T. P. DiLorenzo. 2008. Rapid identification of MHC class I-restricted antigens relevant to autoimmune diabetes using retrogenic T cells. *J. Immunol. Methods* 335: 106–115.
32. Mukhopadhaya, A., T. Hanafusa, I. Jarchum, Y. G. Chen, Y. Iwai, D. V. Serreze, R. M. Steinman, K. V. Tarbell, and T. P. DiLorenzo. 2008. Selective delivery of beta cell antigen to dendritic cells in vivo leads to deletion and tolerance of autoreactive $CD8^+$ T cells in NOD mice. *Proc. Natl. Acad. Sci. USA* 105: 6374–6379.
33. Weinstein, J. S., M. J. Delano, Y. Xu, K. M. Kelly-Scumpia, D. C. Nacionales, Y. Li, P. Y. Lee, P. O. Scumpia, L. Yang, E. Sobel, et al. 2013. Maintenance of anti-Sm/RNP autoantibody production by plasma cells residing in ectopic lymphoid tissue and bone marrow memory B cells. *J. Immunol.* 190: 3916–3927.
34. Xu, Y., P. Y. Lee, Y. Li, C. Liu, H. Zhuang, S. Han, D. C. Nacionales, J. Weinstein, C. E. Mathews, L. L. Moldawer, et al. 2012. Pleiotropic IFN-dependent and -independent effects of IRF5 on the pathogenesis of experimental lupus. *J. Immunol.* 188: 4113–4121.
35. Lee, P. Y., Y. Kumagai, Y. Xu, Y. Li, T. Barker, C. Liu, E. S. Sobel, O. Takeuchi, S. Akira, M. Satoh, and W. H. Reeves. 2011. IL-1α modulates neutrophil recruitment in chronic inflammation induced by hydrocarbon oil. *J. Immunol.* 186: 1747–1754.
36. Chen, J., S. Grieshaber, and C. E. Mathews. 2011. Methods to assess beta cell death mediated by cytotoxic T lymphocytes. *J. Vis. Exp.* (52): 2724.
37. Chen, J., A. M. Gusdon, J. Piganelli, E. H. Leiter, and C. E. Mathews. 2011. mt-Nd2(a) modifies resistance against autoimmune type 1 diabetes in NOD mice at the level of the pancreatic β-cell. *Diabetes* 60: 355–359.
38. Hamaguchi, K., H. R. Gaskins, and E. H. Leiter. 1991. NIT-1, a pancreatic beta-cell line established from a transgenic NOD/Lt mouse. *Diabetes* 40: 842–849.
39. Jackson, S. H., S. Devadas, J. Kwon, L. A. Pinto, and M. S. Williams. 2004. T cells express a phagocyte-type NADPH oxidase that is activated after T cell receptor stimulation. *Nat. Immunol.* 5: 818–827.
40. Chi, H. 2012. Regulation and function of mTOR signalling in T cell fate decisions. *Nat. Rev. Immunol.* 12: 325–338.
41. Intlekofer, A. M., N. Takemoto, E. J. Wherry, S. A. Longworth, J. T. Northrup, V. R. Palanivel, A. C. Mullen, C. R. Gasink, S. M. Kaech, J. D. Miller, et al. 2005. Effector and memory $CD8^+$ T cell fate coupled by T-bet and eomesodermin. [Published erratum appears in 2006 *Nat. Immunol.* 7: 113.] *Nat. Immunol.* 6: 1236–1244.
42. Szabo, S. J., B. M. Sullivan, C. Stemmann, A. R. Satoskar, B. P. Sleckman, and L. H. Glimcher. 2002. Distinct effects of T-bet in TH1 lineage commitment and IFN-gamma production in CD4 and CD8 T cells. *Science* 295: 338–342.
43. Szabo, S. J., S. T. Kim, G. L. Costa, X. Zhang, C. G. Fathman, and L. H. Glimcher. 2000. A novel transcription factor, T-bet, directs Th1 lineage commitment. *Cell* 100: 655–669.
44. Macías-Pérez, M. E., F. Martínez-Ramos, I. I. Padilla-Martínez, J. Correa-Basurto, L. Kispert, J. E. Mendieta-Wejebe, and M. C. Rosales-Hernández. 2013. Ethers and esters derived from apocynin avoid the interaction between p47phox and p22phox subunits of NADPH oxidase: evaluation in vitro and in silico. *Biosci. Rep.* 33: e00055.
45. Kraut, E. H., and A. L. Sagone, Jr. 1981. The effect of oxidant injury on the lymphocyte membrane and functions. *J. Lab. Clin. Med.* 98: 697–703.
46. Gauthier, M. J. 1976. Modification of bacterial respiration by a macromolecular polyanionic antibiotic produced by a marine *Alteromonas*. *Antimicrob. Agents Chemother.* 9: 361–366.
47. Hawkins, B. J., M. Madesh, C. J. Kirkpatrick, and A. B. Fisher. 2007. Superoxide flux in endothelial cells via the chloride channel-3 mediates intracellular signaling. *Mol. Biol. Cell* 18: 2002–2012.
48. Sena, L. A., S. Li, A. Jairaman, M. Prakriya, T. Ezponda, D. A. Hildeman, C. R. Wang, P. T. Schumacker, J. D. Licht, H. Perlman, et al. 2013. Mitochondria are required for antigen-specific T cell activation through reactive oxygen species signaling. *Immunity* 38: 225–236.
49. Pacheco, Y., A. P. McLean, J. Rohrbach, F. Porichis, D. E. Kaufmann, and D. G. Kavanagh. 2013. Simultaneous TCR and CD244 signals induce dynamic down-modulation of CD244 on human antiviral T cells. *J. Immunol.* 191: 2072–2081.
50. Yoshida, S., S. Hong, T. Suzuki, S. Nada, A. M. Mannan, J. Wang, M. Okada, K. L. Guan, and K. Inoki. 2011. Redox regulates mammalian target of rapamycin complex 1 (mTORC1) activity by modulating the TSC1/TSC2-Rheb GTPase pathway. *J. Biol. Chem.* 286: 32651–32660.
51. Li, M., L. Zhao, J. Liu, A. Liu, C. Jia, D. Ma, Y. Jiang, and X. Bai. 2010. Multi-mechanisms are involved in reactive oxygen species regulation of mTORC1 signaling. *Cell. Signal.* 22: 1469–1476.
52. Sarbassov, D. D., and D. M. Sabatini. 2005. Redox regulation of the nutrient-sensitive raptor-mTOR pathway and complex. *J. Biol. Chem.* 280: 39505–39509.
53. Smith-Garvin, J. E., G. A. Koretzky, and M. S. Jordan. 2009. T cell activation. *Annu. Rev. Immunol.* 27: 591–619.
54. Gelderman, K. A., M. Hultqvist, A. Pizzolla, M. Zhao, K. S. Nandakumar, R. Mattsson, and R. Holmdahl. 2007. Macrophages suppress T cell responses and arthritis development in mice by producing reactive oxygen species. *J. Clin. Invest.* 117: 3020–3028.
55. Kwon, J., K. E. Shatynski, H. Chen, S. Morand, X. de Deken, F. Miot, T. L. Leto, and M. S. Williams. 2010. The nonphagocytic NADPH oxidase Duox1 mediates a positive feedback loop during T cell receptor signaling. *Sci. Signal.* 3: ra59.
56. Yu, H., D. Leitenberg, B. Li, and R. A. Flavell. 2001. Deficiency of small GTPase Rac2 affects T cell activation. *J. Exp. Med.* 194: 915–926.
57. Chen, J., A. M. Gusdon, T. C. Thayer, and C. E. Mathews. 2008. Role of increased ROS dissipation in prevention of T1D. *Ann. N. Y. Acad. Sci.* 1150: 157–166.
58. La Torre, D., and A. Lernmark. 2010. Immunology of beta-cell destruction. *Adv. Exp. Med. Biol.* 654: 537–583.
59. Sumida, T., M. Furukawa, A. Sakamoto, T. Namekawa, T. Maeda, M. Zijlstra, I. Iwamoto, T. Koike, S. Yoshida, H. Tomioka, et al. 1994. Prevention of insulitis and diabetes in beta 2-microglobulin-deficient non-obese diabetic mice. *Int. Immunol.* 6: 1445–1449.
60. Esensten, J. H., M. R. Lee, L. H. Glimcher, and J. A. Bluestone. 2009. T-bet-deficient NOD mice are protected from diabetes due to defects in both T cell and innate immune system function. *J. Immunol.* 183: 75–82.
61. Juedes, A. E., E. Rodrigo, L. Togher, L. H. Glimcher, and M. G. von Herrath. 2004. T-bet controls autoaggressive CD8 lymphocyte responses in type 1 diabetes. *J. Exp. Med.* 199: 1153–1162.
62. Sasaki, Y., K. Ihara, N. Matsuura, H. Kohno, S. Nagafuchi, R. Kuromaru, K. Kusuhara, R. Takeya, T. Hoey, H. Sumimoto, and T. Hara. 2004. Identification of a novel type 1 diabetes susceptibility gene, T-bet. *Hum. Genet.* 115: 177–184.
63. Leiding, J. W., and S. M. Holland. 2012. Chronic granulomatous disease. In *GeneReviews.* M. P. Adam, G. M. Mirzaa, R. A. Pagon, S. E. Wallace, L. J. H. Bean, K. W. Gripp, and A. Amemiya, eds. University of Washington, Seattle, WA.
64. International Chronic Granulomatous Disease Cooperative Study Group. 1991. A controlled trial of interferon gamma to prevent infection in chronic granulomatous disease. *N. Engl. J. Med.* 324: 509–516.
65. Martire, B., R. Rondelli, A. Soresina, C. Pignata, T. Broccoletti, A. Finocchi, P. Rossi, M. Gattorno, M. Rabusin, C. Azzari, et al; IPINET. 2008. Clinical features, long-term follow-up and outcome of a large cohort of patients with chronic granulomatous disease: an Italian multicenter study. *Clin. Immunol.* 126: 155–164.

66. Errante, P. R., J. B. Frazão, and A. Condino-Neto. 2008. The use of interferon-gamma therapy in chronic granulomatous disease. *Recent Pat Antiinfect Drug Discov* 3: 225–230.
67. Holland, S. M. 2010. Chronic granulomatous disease. *Clin. Rev. Allergy Immunol.* 38: 3–10.
68. Newhurger, P. E., and R. A. Ezekowitz. 1988. Cellular and molecular effects of recombinant interferon gamma in chronic granulomatous disease. *Hematol. Oncol. Clin. North Am.* 2: 267–276.
69. Armstrong-James, D., I. A. Teo, S. Shrivastava, M. A. Petrou, D. Taube, A. Dorling, and S. Shaunak. 2010. Exogenous interferon-gamma immunotherapy for invasive fungal infections in kidney transplant patients. *Am. J. Transplant.* 10: 1796–1803.
70. Jyonouchi, H., S. Sun, A. Kelly, and F. L. Rimell. 2003. Effects of exogenous interferon gamma on patients with treatment-resistant chronic rhinosinusitis and dysregulated interferon gamma production: a pilot study. *Arch. Otolaryngol. Head Neck Surg.* 129: 563–569.
71. Whitmire, J. K., J. T. Tan, and J. L. Whitton. 2005. Interferon-gamma acts directly on $CD8^+$ T cells to increase their abundance during virus infection. *J. Exp. Med.* 201: 1053–1059.
72. Joshi, N. S., W. Cui, A. Chandele, H. K. Lee, D. R. Urso, J. Hagman, L. Gapin, and S. M. Kaech. 2007. Inflammation directs memory precursor and short-lived effector $CD8^+$ T cell fates via the graded expression of T-bet transcription factor. *Immunity* 27: 281–295.
73. Joshi, N. S., W. Cui, C. X. Dominguez, J. H. Chen, T. W. Hand, and S. M. Kaech. 2011. Increased numbers of preexisting memory CD8 T cells and decreased T-bet expression can restrain terminal differentiation of secondary effector and memory CD8 T cells. *J. Immunol.* 187: 4068–4076.
74. Lighvani, A. A., D. M. Frucht, D. Jankovic, H. Yamane, J. Aliberti, B. D. Hissong, B. V. Nguyen, M. Gadina, A. Sher, W. E. Paul, and J. J. O'Shea. 2001. T-bet is rapidly induced by interferon-gamma in lymphoid and myeloid cells. *Proc. Natl. Acad. Sci. USA* 98: 15137–15142.
75. Smits, H. H., J. G. van Rietschoten, C. M. Hilkens, R. Sayilir, F. Stiekema, M. L. Kapsenberg, and E. A. Wierenga. 2001. IL-12-induced reversal of human Th2 cells is accompanied by full restoration of IL-12 responsiveness and loss of GATA-3 expression. *Eur. J. Immunol.* 31: 1055–1065.
76. Shuvaev, V. V., J. Han, K. J. Yu, S. Huang, B. J. Hawkins, M. Madesh, M. Nakada, and V. R. Muzykantov. 2011. PECAM-targeted delivery of SOD inhibits endothelial inflammatory response. *FASEB J.* 25: 348–357.
77. Vieceli Dalla Sega, F., L. Zambonin, D. Fiorentini, B. Rizzo, C. Caliceti, L. Landi, S. Hrelia, and C. Prata. 2014. Specific aquaporins facilitate Nox-produced hydrogen peroxide transport through plasma membrane in leukaemia cells. *Biochim. Biophys. Acta* 1843: 806–814.
78. Howden, A. J. M., J. L. Hukelmann, A. Brenes, L. Spinelli, L. V. Sinclair, A. I. Lamond, and D. A. Cantrell. 2019. Quantitative analysis of T cell proteomes and environmental sensors during T cell differentiation. *Nat. Immunol.* 20: 1542–1554.
79. Pollizzi, K. N., C. H. Patel, I. H. Sun, M. H. Oh, A. T. Waickman, J. Wen, G. M. Delgoffe, and J. D. Powell. 2015. mTORC1 and mTORC2 selectively regulate $CD8^+$ T cell differentiation. *J. Clin. Invest.* 125: 2090–2108.
80. Pollizzi, K. N., I. H. Sun, C. H. Patel, Y. C. Lo, M. H. Oh, A. T. Waickman, A. J. Tam, R. L. Blosser, J. Wen, G. M. Delgoffe, and J. D. Powell. 2016. Asymmetric inheritance of mTORC1 kinase activity during division dictates $CD8^+$ T cell differentiation. *Nat. Immunol.* 17: 704–711.
81. Zeng, H., and H. Chi. 2017. mTOR signaling in the differentiation and function of regulatory and effector T cells. *Curr. Opin. Immunol.* 46: 103–111.
82. Pollizzi, K. N., and J. D. Powell. 2015. Regulation of T cells by mTOR: the known knowns and the known unknowns. *Trends Immunol.* 36: 13–20.
83. Long, X., Y. Lin, S. Ortiz-Vega, K. Yonezawa, and J. Avruch. 2005. Rheb binds and regulates the mTOR kinase. *Curr. Biol.* 15: 702–713.
84. Long, X., S. Ortiz-Vega, Y. Lin, and J. Avruch. 2005. Rheb binding to mammalian target of rapamycin (mTOR) is regulated by amino acid sufficiency. *J. Biol. Chem.* 280: 23433–23436.
85. Inoki, K., Y. Li, T. Xu, and K. L. Guan. 2003. Rheb GTPase is a direct target of TSC2 GAP activity and regulates mTOR signaling. *Genes Dev.* 17: 1829–1834.
86. Hultqvist, M., P. Olofsson, J. Holmberg, B. T. Bäckström, J. Tordsson, and R. Holmdahl. 2004. Enhanced autoimmunity, arthritis, and encephalomyelitis in mice with a reduced oxidative burst due to a mutation in the Ncf1 gene. *Proc. Natl. Acad. Sci. USA* 101: 12646–12651.